Pergamon

Geochimica et Cosmochimica Acta, Vol. 67, No. 20, pp. 3871–3887, 2003

0016-7037/03 $30.00 + .00

doi:10.1016/S0016-7037(00)00304-1

Iron and sulfide oxidation within the basaltic ocean crust: Implications for chemolithoautotrophic microbial biomass production

WOLFGANG BACH* and KATRINA J. EDWARDS

Department of Marine Chemistry and Geochemistry, Woods Hole Oceanographic Institution, 360 Woods Hole Road, Woods Hole, MA 02543, USA

(*Received October* 3, 2002; revised 28 April 2003; *accepted in revised form April* 28, 2003)

Abstract—Microbial processes within the ocean crust are of potential importance in controlling rates of chemical reactions and thereby affecting chemical exchange between the oceans and lithosphere. We here assess the oxidation state of altered ocean crust and estimate the magnitude of microbial biomass production that might be supported by oxidative and nonoxidative alteration. Compilations of Fe_2O_3, FeO, and S concentrations from DSDP/ODP drill core samples representing upper basaltic ocean crust suggest that $Fe^{3+}/\Sigma Fe$ increases from 0.15 ± 0.05 to 0.45 ± 0.15 within the first 10–20 Myr of crustal evolution. Within the same time frame 70 ± 25% of primary sulfides in basalt are oxidized. With an annual production of 4.0 ± 1.8 × 10^{15} g of upper (500 ± 200 m) crust and average initial concentrations of 8.0 ± 1.3 wt% Fe and 0.125 ± 0.020 wt% S, we estimate annual oxidation rates of 1.7 ± 1.2 × 10^{12} mol Fe and 1.1 ± 0.7 × 10^{11} mol S. We estimate that 50% of Fe oxidation may be attributed to hydrolysis, producing 4.5 ± 3.0 × 10^{11} mol H_2/yr.

Thermodynamic and bioenergetic calculations were used to estimate the potential chemolithoautotrophic microbial biomass production within ridge flanks. Combined, aerobic and anaerobic Fe and S oxidation may support production of up to 48 ± 21 × 10^{10} g cellular carbon (C). Hydrogen-consuming reactions may support production of a similar or larger microbial biomass if iron reduction, nitrate reduction, or hydrogen oxidation by O_2(aq) are the prevailing metabolic reactions. If autotrophic sulfate reduction or methanogenesis prevail, the potential biomass production is 9 ± 7 × 10^{10} g C/yr and 3 ± 2 × 10^{10} g C/yr, respectively. Combined primary biomass production of up to ~1 × 10^{12} g C/yr may be similar to that fueled by anaerobic oxidation of organic matter in deep-seated heterotrophic systems. These estimates suggest that water-rock reactions may support significant microbial life within ridge flank hydrothermal systems, These estimates suggest that water-rock reactions may support significant microbial life within ridge flank hydrothermal systems. *Copyright © 2003 Elsevier Ltd*

1. INTRODUCTION

In recent years it has been suggested that microbial ecosystems that may be harbored within Earth's crustal habits could represent significant unaccounted for reservoirs of biologic carbon and contribute to—or largely control—processes such as mineral weathering and formation of metal sulfide deposits. While these influences are intriguing to speculate about, identifying, quantifying, and otherwise definitively evaluating these hypothesized processes on a global basis remains a daunting task. Unlike near surface environments, it is inherently difficult to directly or indirectly determine the very presence of microorganisms in the crust, let alone assess the community function, structure, or activity in these bare rock systems. The reasons for these difficulties are numerous and include problems associated with access (generally crust must be drilled), contamination (drilling can introduce surface contaminants), and adequate sampling of representative environments (data points are few and far between). These difficulties and the high costs associated with conducting research on crustal ecosystems precludes exploratory studies on any globally significant scale. Rather, future progress will require more rigorously targeted studies that are based on well-reasoned predictions arrived at from theoretical and geochemical studies that may tell us what to look for, where, and why.

An assessment of the potential energy sources that can support chemolithoautrophic microbial ecosystems is important for evaluating possible primary biomass production. Iron (Fe) oxidation (and reduction) and sulfide (S) oxidation are among the potential energy sources for rock-hosted (endolithic) chemoautotrophs within one of the Earth's largest crustal habitats, basalt hosted oceanic aquifers. In addition, Fe oxidation may produce significant amounts of H_2 (Neal and Stanger, 1983; Stevens and McKinley, 2000), which is the principal electron donor for all anaerobic chemolithoautotrophic metabolic pathways (Jannasch, 1995). Broadening our knowledge of the extent and timing of oxidative seawater alteration and the specific oxidation reactions is therefore important for assessing the role of Fe and S oxidation in supporting potential endolithic microbial ecosystems.

Most of the low-temperature alteration of upper ocean crust takes place in the flanks of midocean ridges where 20% of the global heat loss is accomplished by circulation of huge amounts of seawater (Stein et al., 1995). The degree of oxidation of the ocean crust is not well constrained. Fe^{2+} and Fe^{3+} measurements of fresh basalt glass, crystalline interiors of flow units, weathered basalts from the seafloor, and variably altered rocks from the ocean crust suggest that $Fe^{3+}/\Sigma Fe$ increases as a result of cooling and crystallization and later reaction with seawater

* Author to whom correspondence should be addressed (wbach@whoi.edu).

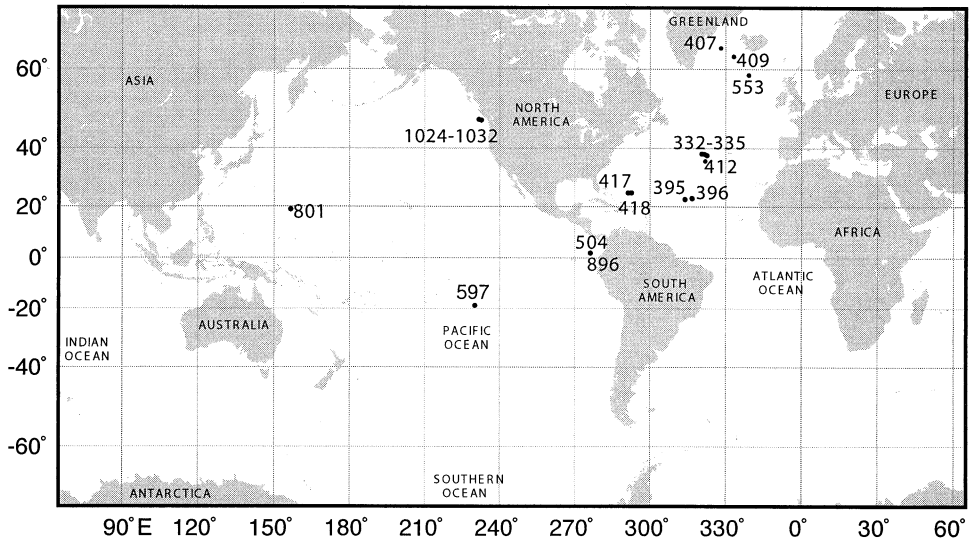

Fig. 1. Location map of DSDP/ODP drill holes included in the compilation of $Fe^{3+}/\Sigma Fe$ and S presented in Table 2.

and seawater-derived hydrothermal fluids (e.g., Alt, 1995a). Holloway and O'Day (2000) estimated hydrogen (H_2) fluxes related to solidification of magma at midocean ridge spreading centers. They suggested that the large amount of H_2released by crystallizing and cooling of rock (300 mol H_2 per cubic meter of rock) may have important implications for chemosynthetic microbial communities associated with axial hydrothermal systems. H_2 produced at lower temperatures (<100°C) by oxidation of Fe^{2+} may be an additional important hydrogen source, although it is debated if such reactions may supply enough $H_2$to support H_2-based subsurface microbial populations (Stevens and McKinley, 1995; Anderson et al., 1998; Stevens and McKinley, 2000, 2001; Anderson et al., 2001). There is mounting evidence that such H_2-based microbial ecosystems may indeed exist on Earth (Stevens and McKinley, 1995; Chapelle et al., 2002); this has important ramifications for the potential for life on other planets.

Reports of textural observations (Fisk et al., 1998; Torsvik et al., 1998; Furnes and Staudigel, 1999) and highly variable carbon isotope measurements (Furnes et al., 2001) raise the possibility of microbial activity within basaltic rocks in off-axis environments. Although these studies did not provide information for how hypothesized microbial communities within the ridge flank crust could function physiologically, recent laboratory studies have provided unequivocal evidence that autotrophic Fe-oxidizing bacteria can grow from the dissolution products of basalt glass (Edwards et al., 2002; Edwards et al., 2003). Finally, a recent study of basement fluids from the Juan de Fuca Ridge flank reveals that microbial life does indeed exist within 3.5 Ma basaltic crust (Cowen et al., 2003).

Here, the geochemical data that currently exist from DSDP and ODP drill cores (Fig. 1) are used to quantify Fe and S oxidation in the flanks of midocean ridges. A maximum chemoautotrophic primary biomass production within ridge flanks is calculated, assuming that (a) microorganisms catalyze the consumption of dissolved oxygen and nitrate to oxidize Fe and S and (b) H_2 is produced by hydrolysis and fuels additional primary production of microbial biomass. These data are discussed in the light of the constraints from biomass production in deep-seated sedimentary systems, basement fluid chemistry, and rock alteration chemistry and mineralogy. The potential global significance of chemoautotrophic primary biomass production in ridge flanks is evaluated and a conceptual model for fluid-microbe-rock interaction in this setting is proposed. We estimate the uncertainties associated with Fe and S oxidation, crustal production rate, depth of oxidative alteration, and energy-biomass conversion efficiency, and let these "errors" propagate through the calculations. These uncertainties are either conservative estimates or standard deviations of mean values (Fe and S concentration).

2. PREALTERATION CONCENTRATIONS AND OXIDATION STATES OF IRON AND SULFUR

2.1. Iron

To determine the extent of Fe oxidation during aging of the ocean crust, average primary Fe content and oxidation state of Fe in pristine midocean ridge basalt (MORB) needs to be known. Melson et al. (2002) report a global average of MORB glass of 8.0 ± 1.3 wt% total Fe (1σ, n = 9050). Determination of the oxidation state (hereinafter expressed as $Fe^{3+}/\Sigma Fe$) of fresh basalt glass is 0.07 ± 0.03, i.e., 7 ± 3% of Fe is ferric (Christie et al., 1986). During cooling and crystallization, ferrous iron in the basaltic liquid reacts with dissolved H_2O to form magnetite (Fe_3O_4) and H_2. Christie et al. (1986) and Bach and Erzinger (1995) compared the Fe oxidation state of glassy rinds with that of flow interiors to determine the amount of oxidation associated with solidification and cooling of lava flows (Table 1). These data indicate that $Fe^{3+}/\Sigma Fe$ increases to 0.15 ± 0.05 in microcrystalline and fine-grained basalt. Using an average total Fe content of 8.0 ± 1.3 wt% and a prealteration oxidation state of 0.15 ± 0.05 the ferrous Fe content of basalt can be estimated at 6.8 ± 1.4 wt%.

It is important to note, however, that these are average rock

Table 1. $Fe^{3+}/\Sigma Fe$ in basaltic glass, microcrystalline transition zone, and crystalline interiors of young basalt flows.

Glass	Microcryst	Fine grained	Reference
0.075	0.077	0.182	Christie et al. (1986)
0.101	0.148	0.195	Christie et al. (1986)
0.114	0.131	0.155	Bach and Erzinger (1995)

values and that Fe contents and $Fe^{3+}/\Sigma Fe$ of different phases are variable. Basaltic glass is not affected by Fe oxidation due to cooling and crystallization. Although volumetrically a minor component of the ocean crust, glass alters at a much faster rate than plagioclase and clinopyroxene. Olivine alteration is also rapid in the deep sea, but, like glass, olivine comprises no more than a few percent of the basaltic crust.

2.2. Sulfur

In MORB magmas, the speciation of sulfur is dominated by sulfide that has a strong affinity to FeO in the melt. Consequently, the solubility of S in basaltic melts is strongly controlled by the concentration of Fe and the redox state of the melt (Mathez, 1976; Wallace and Carmichael, 1992). Because degassing of SO_2 is inhibited under the pressures at the seafloor (Carroll and Webster, 1995), sulfur loss during cooling and crystallization of lava flows is insignificant. This is confirmed by constant S concentration data for pairs of glassy rinds and flow interiors (Bach and Erzinger, 1995). The following empirical relationship between total Fe and S concentrations was established by Mathez (1979) for sulfide-saturated MORB:

$$S\ [wt\%] = 0.023\ Fe\ [wt\%] - 0.059 \quad (1)$$

MORB lavas are usually sulfide saturated (Mathez, 1976; Wallace and Carmichael, 1992), and if differences in the oxygen and sulfur fugacities of MORB magmas can be neglected, this relationship can be used to determine preoxidative sulfur contents on the basis of Fe contents. Assuming negligible uncertainties in Eqn. 1, the sulfur concentration corresponding to a global MORB average of 8.0 ± 1.3 wt% Fe is 0.125 ± 0.020 wt% S.

3. DISTRIBUTION, INTENSITY, AND TIMING OF Fe AND S OXIDATION

The uppermost 200–500 m of basaltic ocean crust are characterized by high permeabilities (10^{-12}-10^{-15} m^2) that facilitate the circulation of large quantities of seawater (Fisher, 1998; Fisher and Becker, 2000). Basaltic rocks react with oxygenated deep-sea water to form secondary minerals, including Fe-oxyhydroxides, smectite, and celadonite (Honnorez, 1981; Alt, 1995a). These phases replace glass, olivine, metal sulfides, and to lesser extents plagioclase and clinopyroxene, and they fill fractures and void space in the crust.

3.1. Spatial Distribution

The extent of oxidation associated with low-T alteration is extremely variable at different spatial scales. Zoned oxidation halos along clay/carbonate/oxyhydroxide filled veins are common (Alt et al., 1996b; Teagle et al., 1996; Marescotti et al., 2000) and indicate diffusion-limited transport in the fairly impermeable rock away from the main fluid pathway. The redox conditions in the pore fluid away from the main fractures change rapidly resulting in precipitation of a variety of Fe-bearing minerals that range from ferric oxides and hydroxides to celadonite and Mg-rich saponite to Fe-rich saponite and pyrite (Marescotti et al., 2000). On a larger scale, highly permeable lithologies, such as brecciated pillow basalts and buried talus fields, effectively channelize fluid flow (Donnelly et al., 1979; Pezard and Anderson, 1989; Bach et al., 2003a). Consequently, these lithologies are much more altered than

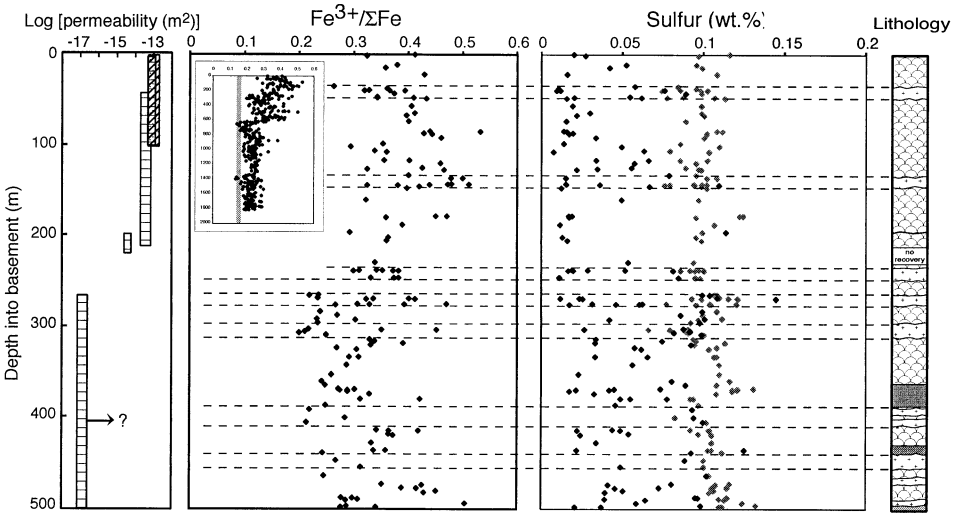

Fig. 2. Downhole profiles of $Fe^{3+}/\Sigma Fe$ and S in Hole 504B down to 500 m subbasement. The inset shows the complete profile for Hole 504B with a preoxidative $Fe^{3+}/\Sigma Fe$ of 0.15 marked by a vertical gray line. Gray symbols are prealteration sulfur contents calculated (see text). Dashed lines mark positions of massive lava flows that are typically less oxidized. Permeability data are from Fisher (1998).

Table 2. Average FeO^{total}, $Fe^{3+}/\Sigma Fe$, and S for deep boreholes in basaltic ocean crust.

Leg	Site	Hole	Latitude	Longitude	Water depth (m)	Sediment thickness (m)	Basement penetration (m)	Recovery (%)	Crustal age (Myrs)	Lithology
37	332	332A	36052.72′N	33038.46′W	1851	104	331	10	3.5	Basalt, basalt breccis, interlayered sediments
37	332	332B	36052.72′N	33038.46′W	1983	149	583	21	3.5	Basalt, basalt breccia
37	333	333A	36050.45′N	33040.05′W	1666	219	310	8	3.5	Basalt, basalt breccia
37	334	334	37002.13′N	34024.87′W	2619	260	124	20	9.5	Basalt overlying a gabbra-peridotite sequence
37	335	335	37017.74′N	35011.92′W	3188	454	108	38	15	Pillow basalt
45	395	395A	22045.35′N	46004.90′W	4485	111	577	18	7.3	Basalt and breccia
45	396	396	22058.88′N	43030.95′W	4450	126	96	33	9	Pillow basalt
46	396	396B	22059.14′N	43030.90′W	4459	151	255	23	13	Basalt and breccia
49	407	407	63056.32′N	30034.56′W	2493	282	177	25	35	Basalts, volcanic breccia, and interlavered sediment
49	409	409	62036.98′N	25057.17′W	834	80	239	25	2.4	Basalt
49	412	412A	36033.74′N	33009.96′W	2626	163	131	18	1.6	Basalt flows and intercalating limestone
51–53	417	417A	25006.63′N	68002.48′W	5478	208	209	61	118	Basalt and breccia
51–53	417	417D	25006.69′N	68002.81′W	5489	343	366	70.2	118	Basalt
51–53	418	418A	25002.10′N	68003.44′W	5519	324	544	72	118	Basalt
51–53[a]	417/418								118	
81	553	553A	56005.32′N	23020.61′W	2339	499	183	50	59	Basalt
92	597	597C	18048.43′S	129046.22′W	4164	53	91	53	29	Massive basalt flows
129	801	801C	18038.54′N	156021.59′E	5685	494	101	60.2	170	Basalt
69–148[b]	504	504B	1013.611′N	83043.818′E	3474	270	1,841	20.1	6.6	Pillowed and massive basalt, breccias
69–148[c]	504	504B							6.6	
148	896	896A	1013.01′N	83043.39′W	3459	200	269	26.9	6.6	Basalt
168	1024	1024B	47054.27′N	128045.13′W	2614	168	12	25	1	Basalt
168	1025	1025C	47053.25′N	128038.92′W	2606	106	41	36.9	1.2	Basalt
168	1026	1026B	47045.76′N	127045.55′W	2658	256	39	5	3.5	Basalt and breccia
168	1027	1027C	47045.39′N	127043.87′W	2667	606	26	45	3.6	Basalt and diabase sill
168	1032	1032A	47046.77′N	128007.34′W	2656	290	48	31	2.6	Basalt

[a] Super-composite for ODP Sites 417 and 418 from Staudigel et al. (1996).
[b] Only data for uppermost 500 m were used.

massive flow units that are impermeable and less susceptible to oxidation. $Fe^{3+}/\Sigma Fe$ of oxidatively altered brecciated rocks can be as high as 0.95 (Thompson, 1983), while that of massive flow interiors is only slightly elevated. This variability at different spatial scales makes it extremely difficult to quantify the extent of Fe oxidation in the upper crust.

The 2-km deep DSDP/ODP Hole 504B in 6.6 Ma crust 200 km south of the Costa Rica Rift in the eastern equatorial Pacific serves as the reference section for basaltic ocean crust. The downhole variation in measured $Fe^{3+}/\Sigma Fe$ ratios of rocks from 504B is displayed in Figure 2 (inset). Throughout most of the upper 2 km of basement, the $Fe^{3+}/\Sigma Fe$ is increased above primary and prealteration oxidation states. $Fe^{3+}/\Sigma Fe$ is highest in the uppermost 200 m of crust consistent with the observation of highest permeability in that part of the crust (Fig. 2). The underlying 400 m of volcanics are slightly less oxidized and their alteration style is dominated by interaction with reacted seawater at elevated temperatures (<150°C; Alt et al., 1996a). Apart from this crude division, oxidation of Fe and S is highly variable and does not exhibit systematic trends with depth in the uppermost 500 m (Fig. 2). Large differences in the extent of oxidation exist between and within individual flow units. In general, massive flows appear less oxidized than pillowed and brecciated units, reflecting lower permeability of the massive flows that results in lower time-integrated fluid fluxes (Bach et al., 2003a). Other boreholes show similar relationships between alteration, lithology, and depth but the overall extent of oxidation is greater than in Hole 504B. This discrepancy probably reflects the young basement age and rapid sedimentation rate at Site 504.

3.2. Degree of Fe and S Oxidation

Upper crust of much greater age (118 Ma) has been sampled at Sites 417/418 (e.g., Donnelly et al., 1979). Due to the high core recovery (~70%) these borehole are particularly suitable for deriving chemical budgets of seawater-crust exchange (Hart and Staudigel, 1982; Staudigel and Hart, 1983; Thompson, 1983; Staudigel et al., 1995, 1996). Weighted by lithology and alteration style, the average $Fe^{3+}/\Sigma Fe$ at Sites 417/418 is 0.56 (Staudigel et al., 1996) much greater than the weighted average for Hole 504B ($Fe^{3+}/\Sigma Fe = 0.35$; Bach et al., 2003b). The true average Fe oxidation state of altered crust is probably bracketed by the estimates for 504B and 417/418. Preliminary geochemical data for Hole 801C in Jurassic Pacific crust indicates that the magnitudes of chemical changes are similar to those ob-

Table 2. (Continued)

Alteration intensity	Full spreading rate (mm/yr)	FeO^{total} (wt%)	1σ (wt%)	$Fe^{34}/\Sigma Fe$	1σ	N	[S]obs (wt%)	1σ (wt%)	[S]prim. (wt%)	1σ (wt%)	ES (wt%)	1σ (wt%)
Generally slight	23	9.38	1.13	0.289	0.052	18	0.041	0.034	0.109	0.013	0.068	0.037
Slight to moderate	23	8.28	1.56	0.293	0.077	58	0.041	0.049	0.089	0.017	0.048	0.052
Moderate	23	9.07	1.02	0.318	0.082	62	0.036	0.037	0.103	0.012	0.067	0.039
Slight to moderate	23	8.78	0.56	0.251	0.098	30	0.039	0.037	0.098	0.006	0.059	0.038
Slight to moderate	23	8.99	0.42	0.419	0.094	57	0.040	0.039	0.102	0.005	0.062	0.040
Fresh moderate to high in breccia	25	8.95	1.09	0.322	0.093	59	0.054	0.041	0.101	0.012	0.047	0.043
Slight to moderate	25	8.29	0.26	0.391	0.111	7	0.029	0.016	0.089	0.003	0.060	0.016
Mostly fresh to slight	25	8.88	0.82	0.328	0.113	94	0.056	0.037	0.100	0.009	0.044	0.038
Slight to moderate	23	12.09	1.25	0.366	0.065	14						
Slight	23	10.67	0.55	0.295	0.073	33						
Slight	23	9.18	0.38	0.194	0.032	20						
High to complete	25	8.85	0.86	0.434	0.092	15						
Slight to moderate	25	9.60	0.80	0.450	0.080	91						
Slight to moderate	25	9.30	0.80	0.400	0.080	220	0.009	0.009	0.107	0.009	0.098	0.013
	25	10.02		0.560								
Slight to moderate	22	12.37	1.02	0.363	0.085	23						
Moderate	130	10.38	1.34	0.341	0.080	60	0.092	0.033	0.127	0.016	0.035	0.037
Slight to high	150	10.26	2.45	0.372	0.147	60						
Slight to complete	60	9.03	1.02	0.347	0.074	154	0.051	0.035	0.103	0.012	0.052	0.037
		9.07		0.331			0.052		0.103		0.051	
Slight to moderate	60	8.51	0.53	0.403	0.105	46	0.053	0.041	0.093	0.006	0.040	0.041
Fresh to moderate	60	9.50	1.00	0.250								
Fresh to moderate	60	9.50	1.00	0.250	0.030							
Slight to moderate (high in breccias)	60	9.86	0.83	0.330	0.040							
Slight to moderate	60	8.92	1.54	0.360	0.040							
Fresh to slight	60	9.50	1.00	0.300	0.040							

[c] Super-composite for volcanic zone in Hole 504B from Bach et al. (2003b). Data were compiled from the Initial Reports and Scientific Result volumes of the respective DSDP/ODP Legs. The full database can be obtained from WB upon request.

served at Sites 417/418 (Kelley et al., 2003), suggesting that average old ocean crust is more intensely altered and oxidized than in Hole 504B. We here assume an average Fe oxidation state of $Fe^{3+}/\Sigma Fe = 0.45 \pm 0.15$ and a corresponding increase in $Fe^{3+}/\Sigma Fe$ from $0.15 \pm 0.05 \times 0.30 \pm 0.16$. With a primary Fe content of 8.0 ± 1.3 wt% (Melson et al., 2002), it follows that 2.4 ± 1.3 wt% Fe is oxidized.

Crust of fairly young age (e.g., Hole 504B) has lost ~50% of its initial sulfur content through oxidation of primary metal sulfides (pentlandite, pyrrhotite, and chalcopyrite) to oxides and oxyhydroxides. Data for Sites 417/418 (Donnelly et al., 1979) suggest ~90% S loss (Table 2). We assume a sulfur loss of $70 \pm 25\%$ and an average primary S content of 0.125 ± 0.020 and estimate that average altered basalt has lost 0.088 ± 0.034 wt% sulfur.

The Fe and S oxidation budgets can be converted to steady-state oxidation rates if the annual mass of basalt that is exposed to oxidation is known. This mass can be estimated from the annual crustal production rate, the depth extent of oxidation, upper crustal porosity, and basalt density. The production rate of ocean crust has been estimated at 3.45 km^2/yr (Parsons, 1981), but with the recent modifications of the magnetic age scale (Cande and Kent, 1995) the actual rate may be considerably lower. The depth extent of oxidative alteration (as indicated by the development of celadonite and Fe-oxyhydroxides) is 310 mbsf in Hole 504B (Honnorez, 1981) and at least 500 m in 417/418 (Furnes and Staudigel, 1999). The porosity of upper ocean crust decreases as a function of time (e.g., Johnson and Semyan, 1994; Carlson, 1998); however, there is still significant porosity and permeability in upper crust of old age (e.g., Fisher, 1998). We assume a seafloor production rate of 3.0 ± 0.5 km^2/yr, a depth extent of oxidation of 500 ± 200 m, an upper crustal porosity of 0.10 ± 0.05, and a basalt density of 2950 ± 50 kg/m^3 to calculate an upper crustal production rate of $4.0 \pm 1.8 \times 10^{12}$ kg/yr. With the Fe and S oxidation budgets estimated above (24 ± 13 g Fe/kg basalt and 0.88 ± 0.34 g S/kg basalt), we calculate global upper ocean crust oxidation rates of $9.6 \pm 6.8 \times 10^{13}$ g Fe/yr ($1.7 \pm 1.2 \times 10^{12}$ mol Fe/yr) and $3.5 \pm 2.1 \times 10^{12}$ g S/yr ($1.1 \pm 0.7 \times 10^{11}$ mol S/yr).

3.3. Timing of Oxidative Alteration

Several lines of evidence indicate that vigorous seawater circulation and oxidative alteration may predominantly take place in young crust. (1) Age dating of celadonite (a ferric mica that forms under mildly oxidizing conditions, e.g., Andrews,

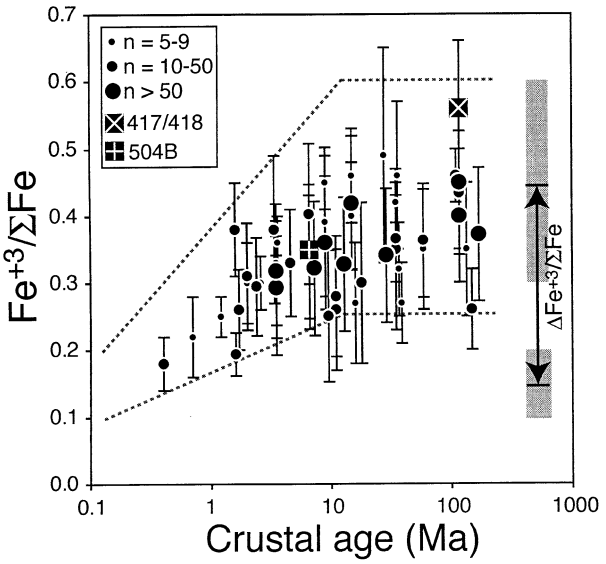

Fig. 3. Plot of average $Fe^{3+}/\Sigma Fe$ of altered basalt samples versus basement age. Data are from Johnson and Semyan (1994) and Table 3. Each circles represents the unweighted average for an entire bore hole with 2σ standard deviation indicated by the error bars. Weighted averages are represented by solid squares. The symbol size varies with the number of analyses available for individual holes (see inset). There is a weak correlation between $Fe^{3+}/\Sigma Fe$ and crustal age suggesting that $Fe^{3+}/\Sigma Fe$ predominantly increases within the first 10 to 20 Myr of crustal evolution.

1979) suggests that oxidative alteration takes place dominantly in the first 10 to 15 myr of crustal evolution (e.g., Hart and Staudigel, 1986; Peterson et al., 1986; Booij et al., 1995). (2) Global heat flow distribution analyses (Stein et al., 1995) indicate that $\sim 3 \times 10^{12}$ W are transported by hydrothermal convection in young ridge flanks (crustal age 1–10 Ma). (3) Bulk permeability of the upper 100 m of basaltic crust formed at nonsedimented, midocean ridges tends to decrease most rapidly within the first few million years of crustal evolution (Fisher and Becker, 2000). (4) Sonic velocities of upper crust increase mainly within the first 10 Myr of crustal evolution, implying that sealing of fractures and voids in upper ocean crust is rapid (e.g., Grevemeyer and Weigel, 1997; Carlson, 1998).

Compilations of $Fe^{3+}/\Sigma Fe$ data for basaltic core samples from drill holes also suggest the extent of oxidative alteration increases chiefly within the first 10 to 20 Myr (Johnson and Semyan, 1994; Fig. 3, Table 2). The considerable scatter in Figure 3 results from (1) effects of various sediment thickness and basement topography (a thick sediment layer and no basement outcrops will shut down circulation early), (2) variable volcanic stratigraphy (pillowed and brecciated flow are often more altered than thick massive flows), (3) regional differences in the concentrations of oxidants in recharging seawater, and (4) biases related to low core recovery and preferential sampling of fresh samples by igneous petrologists versus altered samples by metamorphic petrologists). We realize that these problems are to severe to assess oxidation rates during crustal aging with satisfying accuracy. The compilation is useful, however, as it shows that the oxidation states at the majority of sites are consistent with our estimated oxidation state of altered crust ($Fe^{3+}/\Sigma Fe = 0.45 \pm 0.15$) that is primarily based on two sites (504 and 417/418).

3.4. Agents and Rates of Oxidative Alteration

3.4.1. Sulfate

Sulfate, at 28 mmol/kg, is the most abundant oxidizing agent dissolved in seawater. Lecuyer and Yanick (1999) assumed that Fe oxidation within the ocean crust is governed by sulfate reduction. Rates of abiogenic sulfate reduction, however, are very sluggish at low temperatures (Machel, 2001) and the majority of anhydrite samples from Hole 504B exhibits seawater-like sulfur isotope ratios (Alt et al., 1985) suggesting that significant sulfate reduction at temperatures below 150°C did not take place. Sulfate reduction is thus ruled out as playing a large role in oxidizing Fe in upper oceanic crust, although it may well be important at higher temperatures (Shanks and Seyfried, 1987).

3.4.2. Oxygen and Nitrate

Oxygen dissolved in crustal fluids is commonly assumed to be consumed rapidly during oxidation of ferrous Fe in olivine, clinopyroxene, magnetite, and volcanic glass. Oxidation likely occurs in several stages: dissolution of a ferrous mineral (Eqn. 2), oxidation of Fe^{2+} to Fe^{3+} in solution (Eqn. 3), precipitation of ferric hydroxide (Eqn. 4).

$$FeO + 2\,H^+ = Fe^{2+} + H_2O \quad (2)$$

$$Fe^{2+} + 0.25\,O_2(aq) + H^+ = Fe^{3+} + 0.5\,H_2O \quad (3)$$

$$Fe^{3+} + 3\,H_2O = Fe(OH)_{3,s} + 3\,H^+ \quad (4)$$

Ferric hydroxides may recrystallize into more stable oxyhydroxides or oxides. The net reaction indicates that one mol of oxygen can oxidize four mol of ferrous Fe.

$$FeO + 0.25\,O_2(aq) + 1.5\,H_2O = Fe(OH)_{3,s} \quad (5)$$

Fe oxidation by nitrate:

$$5\,Fe^{2+} + NO_3^- + 6\,H^+ = 5\,Fe^{3+} + 0.5\,N_2(aq) + 3\,H_2O \quad (6)$$

is also energetically favorable ($\Delta G^o = -232$ kJ/mol NO_3^-, T = 10°C) and anaerobic, nitrate-dependent microbial Fe oxidation is known to take place (Straub et al., 1996).

Oxygen and nitrate levels of deep sea waters vary as a consequence of remineralization of organic matter. At 4000 m water depth, $O_2(aq)$ and NO_3^- in North Atlantic deep water are 260 μmol/kg and 20 μmol/kg, respectively, while North Pacific deep water has 140 μmol/kg $O_2(aq)$ and 36 μmol/kg NO_3^- (Broecker and Peng, 1982). For simplicity and acknowledging that most young ridge flanks are between 2500 m and 3000 m water depth, we assume the recharging seawater has uniform concentrations of 100 μmol/kg $O_2(aq)$ and 20 μmol/kg NO_3^-.

It is likely that sulfides become oxidized to soluble sulfate, because sulfur is very efficiently removed from the upper crust. A simplified net reaction suggests that two mol of dissolved oxygen are required to oxidize one mol of sulfidic sulfur.

$$FeS + 2\,O_2(aq) = Fe^{2+} + SO_4^{2-} \quad (7)$$

Sulfide may also be oxidized anaerobically by nitrate (e.g., Kuenen et al., 1992):

$$5\,HS^- + 8\,NO_3^- + 3\,H^+ = 5\,SO_4^{2-} + 4\,N_2 + 4\,H_2O \quad (8)$$

At reduced oxygen levels primary sulfide degradation likely proceeds through several steps with sulfite and thiosulfate as intermediate oxidation products that disproportionate to sulfate and bisulfide (Andrews, 1979). Under these circumstances, the S oxidizing capacity per mol oxygen is lower. For instance, if the reaction is simplified as:

$$2\,FeS + 2.5\,O_2(aq) + 5\,H_2O = 2\,Fe(OH)_3 + HS^- + SO_4^{2-} + 3\,H^+ \quad (9)$$

one mol of O_2 would produce only 0.4 mol of sulfate. The bisulfide would react with Fe^{2+} in solution to form secondary pyrite. More recent work has shown that intermediates of sulfide oxidation may also include polysulfides, polythionates, and elemental sulfur (Schippers and Sand, 1999; Schippers and Jørgensen, 2001) suggesting more complex reaction paths and increased potential for S isotope fractionation (Habicht and Canfield, 2001).

Andrews (1979) noted that reactions of this type result in a S loss (~50%) that coincides with the S loss observed in Hole 504B core and argued for pervasive oxidative alteration. However, many S-depleted basalts lack a shift in sulfur isotopic composition, suggesting that localized bulk dissolution of primary sulfide is also common.

The extent of Fe and S oxidation associated with consumption of dissolved O_2 and nitrate depends on the time-integrated water-to-rock ratios. In numerous studies (e.g., Böhlke et al., 1980; Alt et al., 1986; Hart and Staudigel, 1986; Gillis and Robinson, 1990) chemical mass balance methods were used to estimate water-to-rock mass ratios of several hundred to 1000 for the uppermost 500 m of oceanic crust. A water-to-rock mass ratios of 100, implies that 100 g of seawater (10 μmol O2 and 2 μmol NO_3^-) react with 1 g basalt (1.43 mmol total Fe; 1.22 mmol ferrous Fe) and can oxidize 50 μmol of ferrous Fe (4×10 μmol + 5×2 μmol; Eqns. 5 and 6), increasing $Fe^{3+}/\Sigma Fe$ from 0.15 to 0.18. Clearly, water-to-rock mass ratios on the order of 100 cannot account for oxidation of the upper crust by consumption of dissolved oxygen and nitrate. A water-to-rock mass ratios of 1000 corresponds to an increase in $Fe^{3+}/\Sigma Fe$ from 0.15 to 0.50 and can explain the observed increase from 0.15 ± 0.05 to 0.45 ± 0.15 by oxygen and nitrate consumption. Assuming, for simplicity, the stoichiometry of Eqns. 7 and 8, the oxidizing capacity of seawater at a water-to-rock mass ratio of 1000 would be sufficient to oxidize all primary metal sulfides.

Since a range of geochemically determined water-to-rock mass ratios is so large, this suggests that the mass flux of water (and dissolved oxygen and nitrate) is not well enough constrained to estimate the capacity of S and Fe oxidation. Heat flow constraints will therefore be used in section 3.5 when estimating global averages for Fe and S oxidation.

3.4.3. *Hydrolysis*

Hydrolysis by ferrous Fe in basalt glass and mafic minerals may be responsible for some of the shift in $Fe^{3+}/\Sigma Fe$. Reaction of Fe^{2+} phases with heated seawater to form magnetite can be simplified as:

$$3Fe_2SiO_4 + 2H_2O = 2Fe_3O_4 + 3SiO_2 + 2H_2. \quad (10)$$

This type of reaction is believed to account for the high H_2 concentrations in vent fluids from ultramafic-hosted hydrothermal systems (Holm and Charlou, 2001). But it has also been proposed (Evans and Wanklyn, 1946; Neal and Stanger, 1983) that low-T reaction of water with Fe(II)-bearing phases to secondary products such as ferrihydrite, goethite/lepidocrocite, or hematite may proceed through reactions that can be simplified as:

$$2FeO + 4H_2O = 2Fe(OH)_3 + H_2 \quad (11)$$

$$2FeO + 2H_2O = 2FeOOH + H_2 \quad (12)$$

$$2FeO + H_2O = Fe_2O_3 + H_2. \quad (13)$$

Neal and Stanger (1983) suggested that reactions of type 11 through 13 represent a second stage of Fe^{2+} oxidation following the consumption of dissolved oxygen in the water. Consistent with that suggestion, recent experiments show that H_2-producing reactions do not proceed in the presence of free oxygen (Stevens and McKinley, 2000).

If the oxidation of $1.7 \pm 1.2 \times 10^{12}$ mol FeO (cf. Section 3.2) was related solely to hydrolysis, then $0.85 \pm 0.6 \times 10^{12}$ mol H_2 could be produced per year.

3.5. Constraints from Heat Flow

An independent way of estimating average water-to-rock ratios is to scale crustal production rate to the fluid flux and estimate the latter using heat flow constraints. Heat flow (H) and fluid flow (F) are related by the equation

$$H = F/(c_p \Delta T) \quad (14)$$

where c_p is the heat capacity of seawater (~4 J $g^{-1}K^{-1}$ at temperatures below 200°C; Bischoff and Rosenbauer, 1985) and ΔT is the temperature anomaly of the fluid, i.e., the difference between recharging and discharging fluid. The advective heat loss in ridge flank settings (crustal age 1 to 65 Myr) is ~7 TW (Stein et al., 1995) and corresponds to a seawater flux of 4 to 11×10^{15} kg/yr if it is assumed that the fluids are heated by 5 to 15 °C (Elderfield and Schultz, 1996).

Ocean crust younger than 10 Myr appears to be most affected by oxidative alteration (section 3.3), although heat flow measurements show that seawater continues to circulate in crust much older than 10 Myr (Sclater et al., 1980; Noel, 1985; Stein et al., 1995). Of the 7 TW of heat that is transported by seawater circulation in ridge flanks (Stein et al., 1995; Elderfield and Schultz, 1996) ~3 TW is transported through crust of age 1 to 10 Myr, where the bulk of the oxidation appears to take place.

The dependence of Fe and S oxidation on fluid flux and fluid temperature anomaly for convective heat transport of 3 TW within ridge flanks of crustal age <10 Myr is presented in

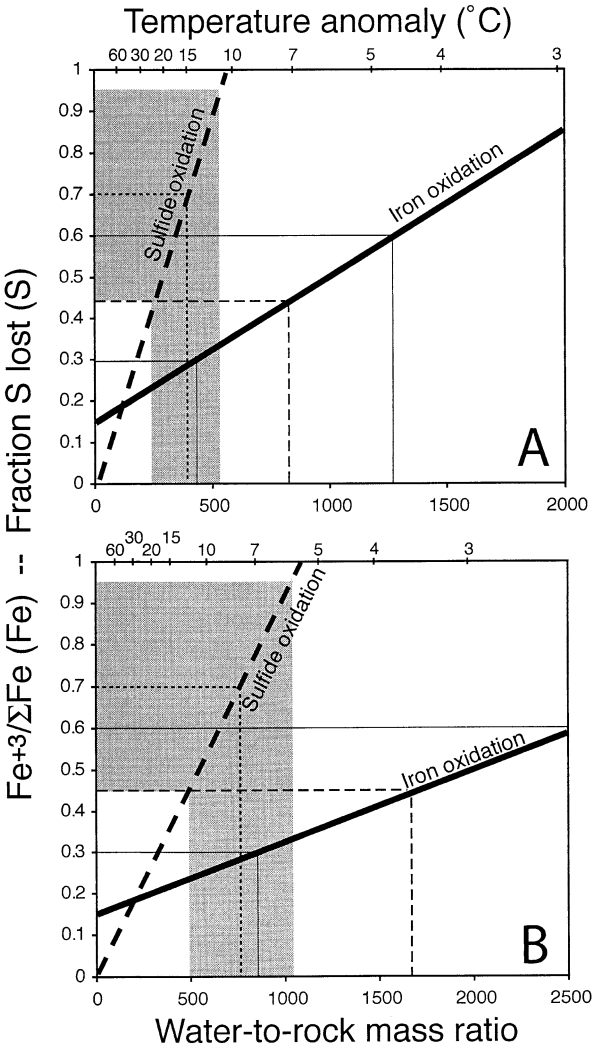

Fig. 4. Dependence of Fe and S oxidation on fluid flux. (A) Fe oxidation only and S oxidation only. (B) Fe and S are simultaneously oxidized at the same rates of oxygen and nitrate consumption. O_2(aq) and NO_3^- concentrations are assumed to be 100 μM and 20 μM, respectively. See text for further explanation.

Figure 4. At water-to-rock mass ratios of <200, a loss of 3 TW can only be achieved if the temperature anomaly of circulating seawater is >30°C. This temperature is lower than observed in bore holes in "warm" ridge flanks, where sediments accumulate rapidly and seal young basement, leading to conductive reheating of the upper basement (Fisher et al., 1990; Mottl and Wheat, 1994; Davis et al., 1999; Wheat and Mottl, 2000). For most ridge flanks, however, basement fluid temperature are probably significantly lower than 30°C (e.g., Elderfield and Schultz, 1996) so that globally averaged water-to-rock mass ratios must be considerably larger.

If only oxidation of Fe is considered, a water-to-rock mass ratio of 860 ± 430 is sufficient to oxidize Fe in the upper crust to $Fe^{3+}/\Sigma Fe$ of 0.45 ± 0.15 and is consistent with heat flow constraints if the average temperature anomaly is $6.9 \pm {}^{6.9}_{2.3}$°C (Fig. 4A). The same fluid flux would provide roughly enough dissolved oxygen and nitrate to the upper crust to oxidize all the S. If it is assumed that Fe and S are oxidized simultaneously and that half of the dissolved oxygen and nitrate are used up to oxidize S while the other half is used up to oxidize Fe (Fig. 4B), $Fe^{3+}/\Sigma Fe$ has increased to 0.29 ± 0.05 when S oxidation has reached 70 ± 25%. This would be achieved at a water-to-rock ratio of 780 ± 280 and a temperature anomaly of $7.6 \pm {}^{4.2}_{2.0}$ °C.

It is very difficult to accurately estimate the H_2-producing potential of Fe oxidation within the ocean crust. We here simply assume that Fe and S are oxidized simultaneously and that both contribute equally to the consumption of dissolved oxygen and nitrate. With this assumption, oxidation from $Fe^{3+}/\Sigma Fe = 0.15$ to $Fe^{3+}/\Sigma Fe \approx 0.30$ is through consumption of dissolved oxygen and nitrate, and further oxidation from $Fe^{3+}/\Sigma Fe \approx 0.30$ to $Fe^{3+}/\Sigma Fe = 0.45$ is through H_2-producing reactions (Fig. 4B). Given a total Fe oxidation rate of 1.7 ± 1.2 × 10^{12} mol/yr, this translates into an Fe oxidation rate 0.9 ± 0.6 × 10^{12} mol/yr and an associated H_2 production rate of 0.45 ± 0.30 × 10^{12} mol H_2.

4. FREE ENERGY CALCULATIONS AND POTENTIAL BIOMASS PRODUCTION

The Fe and S oxidation rates and the H_2 production rate derived in the preceding sections can be used to calculate the amount of geochemical energy available to support chemolithoautotrophic primary production within ridge flanks. The principal behind this approach is outlined in McCollom (2000). A thermodynamic database identical to the one discussed in detail in McCollom (2000) was used to calculate the standard free energies (ΔG^o) for the various redox reactions. The free energies were then calculated according to equation:

$$\Delta G = \Delta G° + RT \ln Q \quad (15)$$

where Q, the activity quotient of the reactants and reaction products, was calculated on the basis of the composition (pH, Na^+, K^+, Ca^{2+}, Mg^{2+}, Cl^-, SO_4^{2-}, HCO_3^-) of basement fluids in ODP Hole 1024 in 1 Ma crust of the eastern Juan de Fuca Ridge flank (Sansone et al., 1998; Elderfield et al., 1999). Concentrations of Fe^{2+}, Fe^{3+}, O_2(aq), H_2(aq), HS^-, and CH_4(aq) are not reported for any ridge flank fluid. The activities of these compounds in basement fluids will strongly control the energetics of potential chemolithoautotrophically catalyzed reactions. The concentrations of both NO_3^- and NH_4^+ are assumed to be 10 μmol/kg; the elevated NH_4^+ concentration is consistent with measurements of basement fluids from Site 1026 on 3.5 Ma eastern Juan de Fuca Ridge flank crust (Cowen et al., 2003). We assume Fe^{2+} to be controlled by fayalite solubility (log $K_{10°C}$ = 20.5, $a_{fayalite}$ = 0.2) and Fe^{3+} by ferrihydrite solubility (log $K_{10°C} = -5.6$, $a_{ferrihydrite} = 1$). HS^- and CH_4(aq) concentrations were assumed to be 20 μmol and 1.25 mmol per kg fluid, similar to deep groundwaters in continental basalts (Chapelle et al., 2002). For oxygen-consuming reactions, O_2(aq) concentration was assumed to be 10^{-5} mol/kg, while H_2(aq) was set to 10 nmol/kg for the H_2-consuming reactions. The effect of varying H_2(aq) concentrations on the free energy of hydrogen-consuming reactions is depicted in Figure 5. Sulfate reduction and methanogenesis are exogenic only above hydrogen activities above $\sim 10^{-11}$ mol/kg and $\sim 10^{-9}$ mol/kg, respectively. Below $\sim 10^{-9}$ mol/kg H_2(aq), iron reduction is energetically more favored than sulfate reduc-

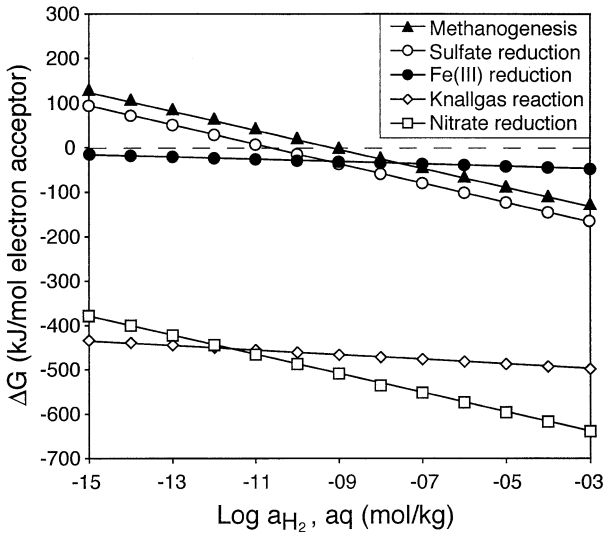

Fig. 5. Dependence of free energy on H_2(aq) activities for various metabolic reactions. See footnote of Table 3 for assumptions. O_2(aq) activity for hydrogen oxidation by O_2(aq) (Knallgas reaction) is assumed to be 10^{-5} mol/kg (solid line) and 10^{-20} mol/kg (dashed line).

tion. Hydrogen oxidation by O_2(aq) (Knallgas reaction) and nitrate reduction have higher energy yields (per mole electron acceptor) than iron reduction, sulfate reduction, and methanogenesis.

The free energy also varies as a function of temperature (Fig. 6). While free energies for all reactions increase as temperature goes up (cf. Eqn. 15), the slopes differ significantly. The free energy for nitrate reduction and methanogenesis show the strongest temperature dependence, while that for sulfate and Fe^{3+} reduction remain fairly constant. With the assumed fluid composition, the energy yields for methanogenesis are fairly small and the free energy becomes positive above a temperature of ~40°C.

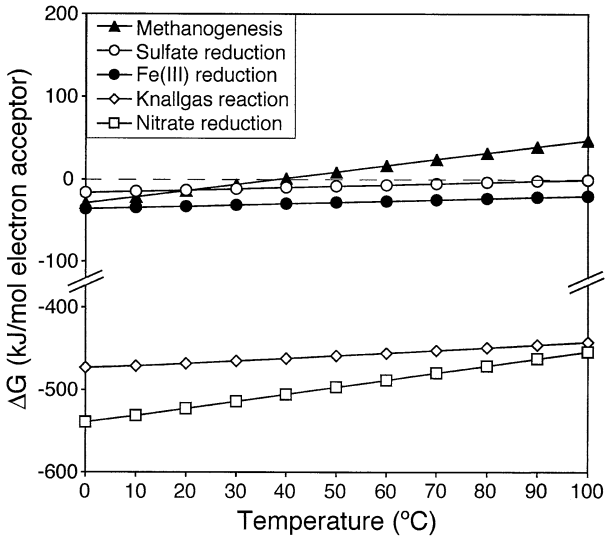

Fig. 6. Temperature dependence of free energy for H_2-consuming reactions (H_2(aq) = 10 nM). O_2(aq) activity for the Knallgas reaction is assumed to be 10^{-20} mol/kg.

Calculating biomass yields for chemoautotrophic growth of microorganisms is not a trivial problem (see reviews in Heijnen and Van Dijken, 1992; Battley, 1998). Many anaerobic bacteria appear to require a minimum of about −20 kJ to exploit the free energy released (Schink, 1997), although there is also evidence that syntropically cooperating anaerobes thrive close to thermodynamic equilibrium (Jackson and McInerney, 2002). Here, the concept of Gibbs energy dissipation (an empirical way of relating chemical energy to chemotrophic biomass production) is used to calculate biomass yields. Heijnen and Van Dijken (1992) observed that the free energy dissipated per amount of produced biomass is chiefly a function of the carbon source and the nature of the electron donor. These authors found that, for autotrophic growth, Gibbs energy dissipation coefficients are around 1000 kJ/mol cellular carbon for electron donors that do not require reversed electron transfer, while they are ~3.5 times greater when reversed electron transport is involved. The uncertainties associated with these Gibbs energy dissipation coefficients are smaller than 40% (Heijnen and Van Dijken, 1992).

Results of the biomass production calculations are presented in Table 3. The potential primary chemolithoautotrophic biomass production by Fe- and S-oxidizers is $48 \pm 21 \times 10^{10}$ g C biomass per year with similar contributions from Fe and S oxidation. H_2-consuming microorganisms may produce a similar or even larger amount of biomass if Fe-reduction ($39 \pm 30 \times 10^{10}$ g C/yr), nitrate-reduction ($73 \pm 56 \times 10^{10}$ g C/yr), or hydrogen oxidation by O_2(aq) ($108 \pm 84 \times 10^{10}$ g C/yr) is the prevailing catabolic reaction, but is predicted to be much smaller if sulfate reduction ($9 \pm 7 \times 10^{10}$ g C/yr) or methanogenesis ($3 \pm 2 \times 10^{10}$ g C/yr) dominate. Combined, a maximum of $>10^{12}$ g cellular carbon may be produced annually on the basis of the estimated Fe and S oxidation and H_2 production rates in ridge flanks. We will show below (section 5.3) that this chemolithoautotrophic primary biomass production may be of the same order of magnitude as that supported by anaerobic degradation of organic matter and that its contribution to carbon cycling in the deep sea may be important.

5. DISCUSSION AND CONCLUSIONS

5.1. Possible Evidence from the Rock Record

Although we assume that oxidative alteration is entirely mediated by microorganisms, it is important to realize that microbial activity does not need to be invoked to explain any of the mineralogical transformations of basalt during weathering. Quantifying the role of microorganisms in crustal alteration is difficult, but it is likely that microbes are present within ridge flank crust, as countless examples illustrate that, given there is fluid flow, deep subsurface microorganisms exploit chemical disequilibrium that it is maintained by sluggish reaction kinetics (e.g., Lovley and Chapelle, 1995; Pederson, 1997).

The actual fraction of ocean crust alteration that is microbially mediated is difficult to constrain, but textural criteria have been developed to distinguish between biogenic and abiogenic alteration (Fisk et al., 1998; Furnes and Staudigel, 1999). Detailed transmission electron microscopy studies (Alt and Mata, 2000; Zhou et al., 2001) have identified marked microscale chemical heterogeneities in altered glass but were unable

Table 3. Results of metabolic energy calculations.

Reaction	Aerobic sulfide oxidation	Anerobic sulfide oxidation	Aerobic Fe (II) oxidation	Anaerobic Fe (II) oxidation	Methanogenesis	Sulfate reduction	Iron reduction	Knallgas reaction	Nitrate reduction
Equation	$HS^- + 2O_2(aq) = SO_4^{2-} + H^+$	$5HS^- + 8NO_3^- + 3H^+ = SO_4^{2-} + N_2 + 4H_2O$	$Fe^{2+} + 0.25\ O_2(aq) + H^+ = Fe^{3+} + 0.5\ H_2O$	$5Fe^{2+} + NO_3^- + 6H^+ = 5Fe^{3+} + 0.5N_2(aq) + 3H_2O$	$HCO_3^- + H^+ + 4H_2(aq) = CH_4(aq) + 3H_2O$	$SO_4^{2-} + H^+ + 4H_2(aq) = HS^- + 4H_2O$	$Fe^{3+} + 0.5\ H_2(aq) = Fe^{2+} + H^+$	$H_2(aq) + 0.5O_2(aq) = H_2O$	$NO_3^- + 4H_2(aq) + H^+ = NH_4^+ + 3H_2O$
Limiting reactant	S (rock)	S (rock)	FeO (rock)	FeO (rock)	H_2(aq)	H_2(aq)	H_2(aq)	H_2(aq)	H_2(aq)
Total S, Fe, H_2 (10^{10} mol/yr)	11 ± 7	11 ± 7	90 ± 60	90 ± 60	45 ± 30	45 ± 30	45 ± 30	45 ± 30	45 ± 30
Stoichiometric factor[a]	0.714	0.286	0.8	0.2					
Corr. S, Fe (10^{10} mol/yr)	7.9 ± 5.0	3.2 ± 2.0	68 ± 45	23 ± 15					
$\Delta G°$ (kJ)[b]	−795	−3785	−51.3	−232	−231	−262	−80.8	−264	−752
ΔG (kJ)[c]	−751	−4087	−66.2	−287	−21.6	−67.6	−36.1	−199	−537.6
ΔG (kJ/mol S, Fe, H_2)	−751	−817.4	−66.2	−57.4	−5.4	−16.9	−72.2	−199	−134.4
Energy (10^{12} kJ/yr)	59 ± 38	25 ± 17	48 ± 30	10 ± 7	2.4 ± 1.6	7.6 ± 5.1	33 ± 22	90 ± 61	60 ± 40
kJ/g C cellular mass[d]	292 ± 117	292 ± 117	292 ± 117	292 ± 117	83 ± 33	83 ± 33	83 ± 33	83 ± 33	83 ± 33
Biomass (10^{10} g C/yr)	20 ± 15	8.8 ± 6.5	16 ± 11	3.5 ± 2.8	2.9 ± 2.2	9.2 ± 7.1	39 ± 30	108 ± 84	73 ± 56
Biomass (10^{10} g dry wt/yr)	44 ± 33	19 ± 14	36 ± 26	7.8 ± 6.1	6.4 ± 4.8	20 ± 16	86 ± 68	237 ± 184	160 ± 123
% anaerobic heterotrophic production[f]	13 ± 10%	5.5 ± 4.0%	10 ± 8%	2.2 ± 1.7%	1.8 ± 1.4%	5.7 ± 4.6%	24 ± 19%	67 ± 52%	45 ± 35%

[a] Based on stoichiometry of reactions and $O_2(aq)/NO_3^-$ molar ratio of 5.

[b] Calculated for T = 10°C and p = 250 bar.

[c] Assumed activities (in mol/kg) of compounds are: $HS^- = 1.8 \times 10^{-b}$, $O_2(aq) = 10^{-5}$, $SO_4^{2-} = 0.014$, $Fe^{2+} = 5.5 \times 10^{-6}$, $Fe^{3+} = 2.5 \times 10^{-18}$, $NO_3^- = 1 \times 10^{-3}$, $NH_4^+ = 1 \times 10^{-3}$, $N_2(aq) = 6 \times 10^{-4}$, $HCO_3^- = 1.6 \times 10^{-8}$, $H_2(aq) = 10^{-3}$, $CH_4(aq) = 1.25 \times 10^{-4}$, pH = 7.75 (see text).

[d] From Heijnen and Van Dijken (1992) with an assumed uncertainty of 40%.

[e] Assuming one g C of biomass is the equivalent of 2.2 g dry weight of cells Battley, 1998.

[f] Anaerobic biomass production in marine sediments calculated from D′Hondt et al. (2002) (see text for details)

Note that the total biomass production supported by microbially catalyzed Fe and S redox reactions is the sum of colums 1 through 4 ($48 \pm 21 \times 10^{10}$ g C/yr), while that fueled by hydrogen consumption depends on the type of prevailing metabolic reaction.

to link these directly to microbial activity. Furnes and Staudigel (1999) have used quantitative textural observations to suggest that up to 75% of the uppermost crust is microbially altered. It is interesting to note that the extent of "bio-alteration" (Furnes and Staudigel, 1999) appears to be established in young crust (~6 Myr) and remains unchanged in crust of older age (>50 Myr). Predominance of microbial processing of basalt alteration in young crust is consistent with results reported here suggesting that biomass production is related to oxidative alteration and hydrolysis that is likely most pronounced in young crust.

Despite recent progress in establishing a role for microbes in basalt alteration, the fractions of Fe and S that are oxidized by microbial action within the ocean crust are unknown. Spontaneous oxidation of Fe^{2+} in solution is probably rapid (on the order of minutes), in particular at neutral pH. However, it has been demonstrated (Emerson and Moyer, 1997, 2002) that neutrophilic Fe-oxidizing bacteria are microaerophilic and thrive in the oxic-anoxic transition where spontaneous Fe oxidation is slow. In fact, up to 80% of Fe^{2+} oxidation in Fe-oxidizing microbial mats may be catalyzed by bacteria (Emerson and Revsbech, 1994) and up to 60% of the iron oxides formed at Loihi Seamount vent sites can be attributed to microbial activity (Emerson and Moyer, 2002). Fe-oxidizing bacteria occur in environments where Fe^{2+} rich fluids are exposed to O_2 (in air or dissolved in water). Mineralized strands of filamentous Fe-oxidizing bacteria (Gallionella, Leptothrix, Sphaerotilus) are commonly described from terrestrial hot springs (Konhauser and Ferris, 1996; Jones et al., 1997) and marine hydrothermal sites (Alt, 1988; Juniper and Fouquet, 1988; Zierenberg and Schiffman, 1990). Fe precipitation rates are very rapid onto bacterial surfaces via heterogeneous surface nucleation (Ghiorse, 1984). The cell walls of bacteria are also known to adsorb a variety of metals, and thus they may control metal mobilities in many low-temperature aqueous systems (Fein et al., 1997). Furthermore, Fe oxyhydroxides can adsorb and/or co-precipitate metals from the surrounding water (German et al., 1990; Boyd et al., 1993). It is hence possible that the precipitation of Fe oxyhydroxides onto bacterial surfaces affects the permeability in the uppermost crust, and chemical fluxes of many metals. While it has historically been uncertain whether these microorganisms derive energy from Fe oxidation to grow autotrophically (Juniper and Tebo, 1995), recent laboratory studies of microbially mediated pyrite and basalt glass degradation have demonstrated that a diverse collection of deep-sea autotrophic Fe-oxidizing bacteria are capable of growth on these substrates (Edwards et al., 2002, 2003).

A role for Fe-oxidizers in the formation of low-temperature hydrothermal oxide deposits has been well established, and it is clear that strong chemical gradients in Fe^{2+} and fO_2 are required. One may speculate that, in ridge flanks rocks, the niches where high concentrations of Fe undergo oxidation may be in wall rock adjacent to fractures that act as conduits for oxygenated seawater. The pore fluid within the rock may acquire high Fe concentrations due to the considerable solubility of olivine and glass. A strong redox gradient may develop between the pore fluid and the fluid in the fracture that may facilitate the occurrence of Fe-oxidizing bacteria in a band roughly parallel to the fracture (Fig. 7). In rocks recovered from upper crustal levels, relicts of this steep transition from oxidizing to reducing

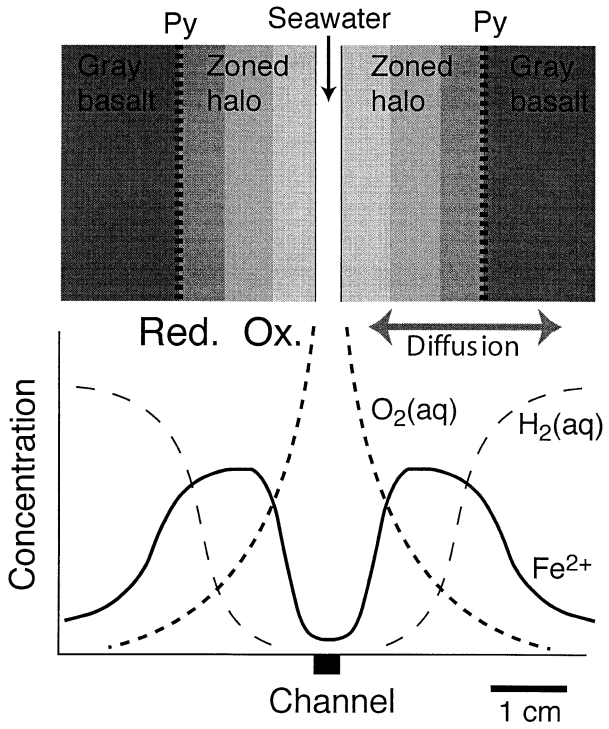

Fig. 7. Simplified view of an alteration halo parallel to a fluid conduit in the upper ocean crust. Oxidizing agents diffuse into the rock, while the pore fluids away from the conduit may become enriched in Fe(II) and H_2 as olivine/glass dissolution and hydrolysis proceed. Fe in the pore water diffuses down the concentration gradient into oxyhydroxide-rich, red bands (Fe-oxidation), leading to a pronounced redistribution of Fe within the alteration halo. As H_2 in the pore water increases away from the fracture, Fe(III) or sulfate may be reduced, possibly leading to the development of black, pyrite-rich bands in the rock.

conditions are often recorded in the form of zoned mm- to cm-wide alteration halos along clay-filled veins that often show a succession of ferric oxyhydroxides, celadonite, saponite, and finally pyrite with an associated change in color from red to brown to dark-gray. Most notably, FeO^{total} is enriched in the oxyhydroxide-rich halo and depleted in the adjacent saponite-rich layer, indicating a net transport of Fe to the oxyhydroxide-rich halo (Marescotti et al., 2000). This transport could be achieved in the opposing chemical gradients of oxygen (diffusing into the rock) and dissolved Fe^{2+}, the concentration of which may be highest away from the fracture where nonoxidative alteration of olivine and glass releases Fe^{2+} to the pore fluid. Neutrophilic, microaerophilic Fe-oxidizing bacteria may take advantage of the sluggish oxidation kinetics of Fe^{2+} at low fO_2 and catalyze oxidation and immobilization of Fe within the reddish, oxyhydroxide-rich halo.

H_2 may be produced during the breakdown of olivine and glass within the rock (Eqns. 11–13). Sulfate-reducing bacteria may exploit the thermodynamic disequilibrium between H_2(aq) and sulfate that diffuses into the rock, or Fe^{3+} reducing microorganisms may use H_2 to drive redox-cycling of Fe. Knallgas bacteria might dwell in regions where O_2 is diffusing in while H_2 is too low for other H_2-consuming metabolic reactions to take place.

Coupled to the redox-cycling of Fe could be that of redox-

sensitive trace metals. For example, *Alteromonas putrefaciens* can grow with H_2 as the sole electron donor and has been shown to be capable of using Fe^{3+} as well as U^{6+} as electron acceptors (Lovley et al., 1991). It is hence possible that the strong enrichment of U in oxidation halos of submarine basalts (Aumento, 1971) and gabbros (Bach et al., 2001) is also a result of microbial activity.

It is intriguing to speculate about such potential links between fluid flow, microbial activity, and rock alteration, but in situ microbiological and geochemical techniques will have to be applied to test these ideas.

5.2. Evidence for Microbial Sulfate Reduction within Ridge Flanks?

The possible extent of microbial sulfate reduction can be examined by reviewing S isotope data for crustal rocks and fluids. The $\delta^{34}S$ of most altered basalts is near 0‰ (Andrews, 1979; Hubberten, 1983; Alt et al., 1989; Alt, 1995b), but isotopically very light values for some pyrite separates ($\delta^{34}S$ as low as −33‰; Krouse et al., 1977) have also been reported. It was suggested that the bulk of the secondary pyrite is likely abiogenic (Andrews, 1979; Hubberten, 1983; Alt et al., 1989; Alt, 1995b) and that the isotopic fractionation reflects Eh-dependent redox reactions and disproportionation of sulfur species (cf. Eqn. 9) during which ^{32}S will be preferentially enriched in the reduced species. However, microbial sulfate reduction cannot be ruled out based on these accounts. Possible microbial sulfate reduction is suggested by isotopically heavy anhydrite ($\delta^{34}S = 34–37‰$) separated from a lava flow in Hole 504B at a depth of ~600 m subbasement (Hubberten, 1983; Alt et al., 1985) and by elevated $\delta^{34}S$ of gypsum from a section of fossil upper basement on Macquarie Island (Alt et al., 2003). The majority of the anhydrite recovered from Hole 504B, however, shows seawater-like S isotopic composition. Hence, while some sulfate reduction is indicated, the extent of sulfate reduction cannot be quantified based on the currently available data.

At first glance, geochemical data for ridge flank fluids recovered from the 3.5 Ma eastern flank of the Juan de Fuca Ridge provide no evidence for methanogenesis or bacterial sulfate reduction, as C isotopes in the bicarbonate depleted fluids are not fractionated (Sansone et al., 1998) and the sulfate depletion can be accounted for by diffusive loss into the overlying sediments (Elderfield et al., 1999). It is possible that C isotope fractionation due to microbial activity is minimal at the elevated temperatures in the basement (62°C; Elderfield et al., 1999). But the temperature is similar in the Idaho basalt aquifer (Chapelle et al., 2002), where the $\delta^{13}C$ of the dissolved inorganic carbon is −2‰, significantly shifted from the composition of the influxing mantle carbon (−7‰). The diffusive sulfate loss model is consistent with radiocarbon ages of the fluids (Elderfield et al., 1999), but microbial sulfate reduction may have occurred if the radiocarbon ages are too high as suggested by (Stein and Fisher, 2000). S isotope analyses of pore fluids from sediments just above the sediment-basement interface (Rudnicki et al., 2001) indeed suggest that the sulfate loss is accompanied by a small shift in $\delta^{34}S$ that could be related to microbial sulfate reduction within the basaltic crust (Fig. 8). The nature of the electron donor (H_2 or organic matter), however, is uncertain.

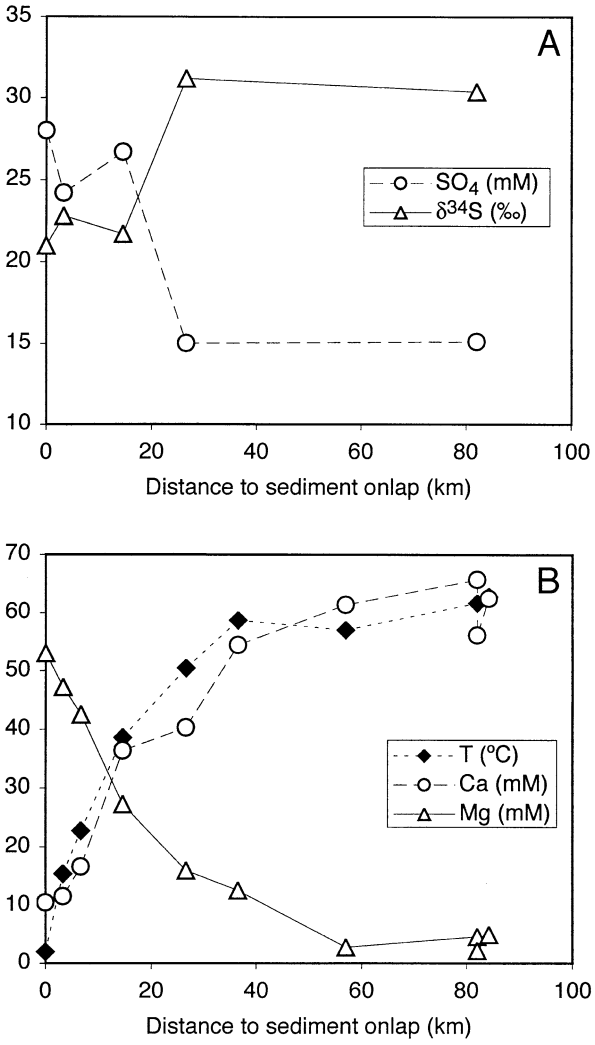

Fig. 8. Near-basement pore-water chemical data plotted against distance to sediment onlap on the eastern Juan de Fuca Ridge flank. (A) Sulfate and $\delta^{34}S$ data from Rudnicki et al. (2001). (B) Ca, Mg, and temperature from Elderfield et al. (1999). Note the shift in S isotopic composition associated with a decrease in basal fluid sulfate concentrations. This shift may be explained by microbial sulfate reduction within the basaltic aquifer. It appears where the increase in fluid temperature and chemical maturation (Ca increase and Mg loss) is most pronounced. It is uncertain if sulfate reduction is driven by oxidation of hydrogen or organic matter.

5.3. Speculations on Hydrogen-Based Microbial Ecosystems within Ridge Flank Crust

The possibility of H_2-based microbial ecosystems has important consequences for the evaluation of habitats for microbial life in the absence of photosynthetic products. In a series of papers (Stevens and McKinley, 1995, 2000, 2001) Stevens and McKinley suggest that H_2 production during water-basalt interaction provides enough H_2 to support a chemolithoautotrophic microbial ecosystem hosted in the Columbia River Basalt

groundwater system. Although, there is considerable debate on whether this ecosystem is driven by abiotic H_2 or traces of organic matter (Anderson et al., 1998; Anderson et al., 2001), a recent report provides new evidence that H_2-based chemolithoautotrophic microbial populations may indeed exist within the Earth's crust (Chapelle et al., 2002). It has even been suggested that H_2 produced within basaltic aquifers may support sulfate-reducing bacteria in carbonates overlying the basalts (Schrag, 1999). The H_2 concentrations of groundwaters in basalt are on the order of nanomoles/kg. Nanomolar-levels of H_2 were detected in abiotic basalt-water reaction experiments, and it appears likely that H_2-production by the mechanisms outlined above may provide sufficient H_2 to support these ecosystems (Stevens and McKinley, 2000).

The maximum steady state H_2 production in ridge flanks is $<9 \times 10^{11}$ mol H_2/yr (assuming all Fe is oxidized by hydrolysis) and may be on the order 4.5×10^{11} mol H_2/yr (see section 3.4). This flux of H_2 is diluted by circulation of vast amounts of seawater, on the order of several 10^{15} kg/yr. At a water-to-rock mass ratio of 1000 ($4.0 \pm 1.8 \times 10^{15}$ kg seawater circulate through ridge flanks per year), a flux of 4.5×10^{11} mol H_2/yr corresponds to average H_2 concentrations in ridge flank fluids of $\sim$100 μmol H_2/kg. H_2 levels in fluids from terrestrial basalt-groundwater systems that may harbor H_2-based microbial communities (Stevens and McKinley, 1995; Chapelle et al., 2002) are four orders of magnitude lower. This suggests that enough H_2 may be produced within ridge flanks to support H_2-based microbial ecosystems (Table 3). The H_2 concentration is particularly critical as it relates to the terminal metabolic reaction in the system (Lovley and Goodwin, 1988; Hoehler et al., 1998). For instance, setting H_2(aq) to 10 nmol/kg in the calculation presented in Table 3 makes methanogenesis energetically favorable. But should nitrate-, sulfate-, or Fe-reducers be present, they would keep the H_2 levels low and would hence thermodynamically inhibit methanogens (Hoehler et al., 1998). In general, nitrate-, sulfate-, or Fe-reduction appears to be more favorable than methanogenesis, even when it is taken into consideration that minimum energy requirement for methanogens is somewhat lower than that of sulfate reducers (Hoehler et al., 1998; Hoehler et al., 2001). The "Knallgas" reaction has the greatest energy yields (Table 3) but only if H_2(aq) and O_2(aq) are both present in significant amounts.

It remains uncertain how much H_2 may be introduced into ridge flank systems, either through serpentinization or by diffusion out of the mantle. Also, the relative importance of the different primary phases in producing H_2 is not well known. Experiments by Stevens and McKinley (2000) suggest that reaction of water with olivine produces H_2 at rates that are much faster than pyroxenes and feldspars. Reaction of olivine-rich lithologies, such as picritic lava flows and mantle peridotites, with seawater may provide subseafloor environments with H_2 fluxes that are high enough to support H_2-based microbial ecosystems. This conclusion is consistent with the carbon isotopic compositions of altered basalt (Furnes et al., 2001) that suggest that methanogens do not seem to be common in ridge flanks. Furnes et al. (2001) find evidence for some methanogenic activity in rocks from slow-spread crust and argue that serpentinization may be required to provide the large quantities of H_2 required by methanogens. Alternatively to supplying H_2 from serpentinization reactions at depths, the large abundance of olivine phenocrysts (Bryan, 1983) in lavas from slow-spread crust may result in larger production of H_2 than in intermediate- and fast-spread crust where olivine phenocrysts are generally less common.

Methanogenesis has lower energy yields than sulfate reduction, unless sulfate concentrations in the circulating seawater are decreased by orders of magnitudes. Evidence for bacterial sulfate reduction is overwhelming in oceanic serpentinites (Alt and Shanks, 1998) but more difficult to discern in altered basalts (Alt, 1995b). Again, this may relate to the production of large quantities of H_2 during peridotite-water interaction that may support a mass of sulfate reducers that is large enough to leave unequivocal traces in the rock record.

We are just beginning to appreciate the global relevance of peridotite-hosted hydrothermal systems (German et al., 1998; Kelley et al., 2001; Bach et al., 2002). The large production of H_2 within these systems make them likely places for significant chemolithoautotrophic primary production.

5.4. Significance of Biomass Production in Ridge Flanks

Oxidation of Fe, S, and H_2 within the upper ocean crust, if entirely mediated by microorganisms, may support the production of a significant microbial biomass ($\sim 10^{12}$ g cellular carbon per year). This it is a remarkably large production for a system that is nominally devoid of organic matter. Recent estimates of subsurface microbial activity in marine sediments suggest that anaerobic methane oxidation ($\Delta G \sim -22.4$ kJ/mol SO_4; Sørensen et al., 2001) prevails (D'Hondt et al., 2002). Using the sulfate flux reported by D'Hondt et al. (2002), at $<42 \times 10^{-3}$ mol/m^2/yr for ocean margin sites and $<13 \times 10^{-5}$ mol/m^2/yr for open-ocean sites, and the areas of these regions respectively (2×10^{14} m^2 and 1.5×10^{14} m^2), biomass production can be calculated. Assuming a Gibbs energy dissipation coefficient for methane oxidizers of 84 kJ per g of cellular carbon (Heijnen and Van Dijken, 1992), the calculated microbial biomass production driven by anaerobic methane oxidation is $<1.6 \times 10^{12}$ g/yr in ocean margins and $<8 \times 10^9$ g/yr in the open ocean. Our results suggest that chemolithoautotrophic biomass production within the basaltic crust may be comparable to that in deep-seated heterotrophic systems (Table 3).

Additional sources for biomass production may exist if degradation of dissolved organic matter or organic synthesis takes place in ridge flank aquifers (Karl, 1995). An unknown fraction of the refractory dissolved organic matter in deep seawater (40 μmol/kg) may be converted to organic compounds that heterotrophs may thrive on. If it is assumed that 40 μmol/kg of dissolved organic carbon is processed through fermentation or respiration reactions that yield an average free energy of -100 kJ/mol C, a water flux of 5×10^{15} kg would mean that 2×10^{11} mol organic matter may be fluxed through ridge flanks per year yielding a free energy on the order of 2×10^{13} kJ. Gibbs energy dissipation coefficients for anaerobic growth of heterotrophic microorganisms are highly variable but center around 40 kJ/g cellular C (Heijnen and Van Dijken, 1992), suggesting that microbial growth on dissolved organic carbon in ridge flanks may produce up to $\sim 5 \times 10^{11}$ g C biomass per year. Hence, unless hydrocarbons are produced within the aquifer (Shock, 1992) or are introduced from below (Gold, 1992),

organic matter-driven biomass production may not exceed the biomass potentially produced lithoautotrophically. Advective and diffusive exchange with sediment pore waters may introduce dissolved organic matter into basaltic aquifers in ridge flanks to a likely small (but basically unknown) extent. Cowen et al. (2003) have recently reported evidence for microbial activity (including sulfate and nitrate reduction) within the Juan de Fuca Ridge flank hydrothermal system that is possibly driven by sediment-derived organic matter. Measurements of organic compounds in ridge flank basement fluids are of critical importance to assess the likelihood of microbial organic matter degradation for driving redox cycling of metals.

How would the proposed microbial activity affect the carbon budget of ridge flank rocks and fluids? If $\sim 10^{12}$ g (8×10^{10} mol) cellular carbon annually produced by chemolithoautotrophs were subject to anaerobic respiration, 4×10^{10} mol CO_2 ($CH_2O = 0.5\ CO_2 + 0.5\ CH_4$) would be produced per year. This amounts to only $<0.4\%$ of the dissolved inorganic carbon fluxed through the ridge flanks per year ($>4 \times 10^{15}$ kg $\times$ 0.0024 mol/kg). The calculated biomass production rates are thus not inconsistent with the observation that carbon isotopic signatures of the majority of calcite veins from the upper ocean crust lack biogenic signatures (e.g., Alt et al., 1996b). However, Furnes et al. (2001) suggested that microbial signatures can be detected in bulk-rock $\delta^{13}C$ compositions of altered basalt glass that contains only traces of carbonate.

The biomass estimates presented in this paper represent maximum values given the range of input values used for the calculations, because it is assumed that the geochemical reactions are entirely microbially mediated. In addition, the Gibbs energy dissipitation values adopted from (Heijnen and Van Dijken, 1992), may not be applicable to very low growth rates where a large fraction of the energy is used up for maintenance processes rather than growth. However, our calculations do not strictly represent maximum values in as far as final compositions are used with calculated initial values to derive a rate that reflects single transformations, and not the dynamic range of redox transformations that could occur.

While our results suggest that chemolithoautotrophic primary production in bare rock systems may be considerable, iterative theoretical and empirical field studies will be required before the magnitude of biomass production in these systems can be tighter constrained.

Acknowledgments—We thank Tom McCollom, Dan Rogers, Meg Tivey, Susan Humphris, Kai Hinrichs, Steve D'Hondt, Jeff Alt, Hubert Staudigel, and David Vanko for discussions. Art Spivack, Axel Schippers, and Hubert Staudigel provided very helpful comments and suggestions. This work was supported by J. Lamar Worzel and Penzance Endowed Funds, the Sidney J. Weinberg Jr. Foundation, the Deep Ocean Exploration Institute at WHOI, and by NSF grants OCE-9811209 (to WB) and OCE-0096992 (to KJE). WHOI contribution number 10801.

Associate editor: D. Canfield

REFERENCES

Alt J. C. (1988) Hydrothermal oxide and nontronite deposits on seamounts in the eastern Pacific. *Mar. Geol.* **81**, 227–239.

Alt J. C. (1995a) Subseafloor processes in mid-ocean ridge hydrothermal systems. In *Seafloor Hydrothermal Systems*, Vol. Geophysical Monograph (eds. S. E. Humphris, R. A. Zierenberg, L. S. Mullineaux, and R. E. Thomson), pp. 85–114. American Geophysical Union.

Alt J. C. (1995b) Sulfur isotope profile through the oceanic crust: Sulfur mobility and seawater-crustal sulfur exchange during hydrothermal alteration. *Geology* **23**, 585–588.

Alt J. C., Saltzman E. S., and Price D. A. (1985) Anhydrite in hydrothermally altered basalts: Deep Sea Drilling Project Hole 504B, Leg 83. In *Initial Reports of the Deep Sea Drilling Project*, Vol. 83 (eds. R. N. Anderson et al.), pp. 283–288. U.S. Government Printing Office.

Alt J. C., Honnorez J., Laverne C., and Emmermann R. (1986) Hydrothermal alteration of a 1 km section through the upper oceanic crust. DSDP Hole 504B: Mineralogy, chemistry and evolution of seawater-basalt interactions. *J. Geophys. Res.* **91**, 309–335.

Alt J. C., Anderson T. F., and Bonnell L. (1989) The geochemistry of sulfur in a 1.3 km section of hydrothermally altered oceanic crust, DSDP Hole 504B. *Geochim. Cosmochim. Acta* **53**, 1011–1023.

Alt J. C., Laverne C., Vanko D., Tartarotti P., Teagle D. A. H., Bach W., Zuleger E., Erzinger J., and Honnorez J. (1996a) Hydrothermal alteration of a section of upper oceanic crust in the eastern equatorial Pacific: A synthesis of results from DSDP/ODP Legs 69, 70, 83, 111, 137, 140, and 148 at Site 504B. In *Proceedings of the Ocean Drilling Program, Sci. Results 148* (eds. J. C. Alt, H. Kinoshita, L. B. Stokking, and P. J. Michael), pp. 417–434. Ocean Drilling Program.

Alt J. C., Teagle D. A. H., Laverne C., Vanko D., Bach W., Honnorez J., and Becker K. (1996b) Ridge flank alteration of upper oceanic crust in the eastern Pacific: A synthesis of results for volcanic rocks of Holes 504B and 896A. In *Proceedings of the Ocean Drilling Program, Sci. Results 148* (eds. J. C. Alt, H. Kinoshita, L. B. Stokking, and P. J. Michael), pp. 435–450. Ocean Drilling Program.

Alt J. C. and Shanks W. C. (1998) Sulfur in serpentinized oceanic peridotites: Serpentinization processes and microbial sulfate reduction. *J. Geophys. Res.* **103**, 9917–9929.

Alt J. C. and Mata P. (2000) On the role of microbes in the alteration of submarine basaltic glass: A TEM study. *Earth Planet. Sci. Lett.* **181**, 301–313.

Anderson R. T., Chapelle F. H., and Lovley D. R. (1998) Evidence against hydrogen-based microbial ecosystems in basalt aquifers. *Science* **281**, 976–977.

Anderson R. T., Chapelle F. H., and Lovley D. R. (2001) Comment on "Abiotic controls on H_2 production from basalt-water reactions and implications for aquifer biogeochemistry." *Environ. Sci. Technol.* **35**, 1556–1557.

Andrews A. J. (1979) On the effect of low-temperature seawater-basalt interaction on the distribution of sulfur in oceanic crust, Layer 2. *Earth Planet. Sci. Lett.* **46**, 68–80.

Aumento F. (1971) Uranium content of mid-ocean ridge basalts. *Earth Planet. Sci. Lett.* **11**, 90–94.

Bach W. and Erzinger J. (1995) Volatile components in basalts and basaltic glasses from the EPR at 9°30′N. In *Proceedings of the Ocean Drilling Program, Sci. Results 142* (eds. R. Batiza, M. A. Storms, and J. F. Allan), pp. 23–29. Ocean Drilling Program.

Bach W., Alt J. C., Niu Y., Humphris S. E., Erzinger J., and Dick H. J. B. (2001) The geochemical consequences of late-stage low-grade alteration of lower ocean crust at the SW Indian Ridge: Results from ODP Hole 735B (Leg 176). *Geochim. Cosmochim. Acta* **65**, 3267–3287.

Bach W., Banerjee N. R., Dick H. J. B., and Baker E. T. (2002) Discovery of ancient and active hydrothermal deposits along the ultraslow spreading Southwest Indian Ridge 10–16°E. *Geochem. Geophys. Geosyst.* **3(7),** 10.1029/2001GC000279.

Bach W., Humphris S. E., and Fisher A. T. (2003a) Water-rock reactions and fluid-flow in the oceanic crust: Reconciling geological, geochemical and geophysical observations. In *Subseafloor Biosphere at Mid-Ocean Ridges* (eds. W. Wilcock, C. Cary, E. DeLong, D. Kelley, and J. Baross). American Geophysical Union. In press.

Bach W., Peucker-Ehrenbrink B., Hart S. R., and Blusztjan J. S. (2003b) Geochemistry of hydrothermally altered oceanic crust: DSDP/ODP Hole 504B – Implications for seawater-crust exchange budgets and Sr- and Pb-isotopic evolution of the mantle. *Geochem. Geophys. Geosyst.* **4(3),** 10.1029/2002GC000419.

Battley E. H. (1998) The development of direct and indirect methods for the study of the thermodynamics of microbial growth. *Thermochim. Acta* **309**, 169–171.

Bischoff J. L. and Rosenbauer R. J. (1985) An empirical equation of state for hydrothermal seawater (3.2 percent NaCl). *Am. J. Sci.* **285**, 725–763.

Böhlke J. K., Honnorez J., and Honnorez-Guerstein B.-M. (1980) Alteration of basalts from Site 396B, DSDP: Petrographic and mineralogic studies. *Contrib. Mineral. Petrol.* **73**, 341–364.

Booij E., Gallahan W. E., and Staudigel H. (1995) Ion-exchange experiments and Rb/Sr dating on celadonites from the Troodos ophiolite, Cyprus. *Chem. Geol.* **126**, 155–167.

Boyd T., Scott S. D., and Hekinian R. (1993) Trace element patterns in Fe-Si-Mn oxyhydroxides at three hydrothermally active seafloor regions. *Res. Geol. Spec. Issue.* **17**, 83–95.

Broecker W. S. and Peng T.-H. (1982) *Tracers in the Sea.* Lamont-Doherty Geological Observatory.

Bryan W. B. (1983) Systematics of model phenocryst assemblages in submarine basalts: Petrologic implications. *Contrib. Mineral. Petrol.* **83**, 62–74.

Cande S. C. and Kent D. V. (1995) Revised calibration of the geomagnetic polarity timescale for the Late Cretaceous and Cenozoic. *J. Geophy. Res.* **100**, 6093–6095.

Carroll M. R. and Webster J. D. (1995) Solubilities of sulfur, noble gases, nitrogen, chlorine, and fluorine in magmas. In *Volatiles in Magmas*, Vol. 30 (eds. M. R. Carroll and J. R. Holloway), pp. 231–279. Mineralogical Society of America.

Chapelle F. H., O'Neill K., Bradley P. M., Methé B. A., Ciufo S. A., Knobel L. L., and Lovley D. R. (2002) A hydrogen-based subsurface microbial community dominated by methanogens. *Nature* **415**, 312–315.

Christie D. M., Carmichael I. S. E., and Langmuir C. H. (1986) Oxidation states of mid-ocean ridge basalt glasses. *Earth Planet. Sci. Lett.* **79**, 397–411.

Cowen J. P., Giovannoni S. J., Kenig F., Johnson H. P., Butterfield D. A., Rappe M. S., Hutnak M., and Lam P. (2003) Fluids from aging ocean crust that support microbial life. *Science* **299**, 120–123.

D'Hondt S. D., Rutherford S., and Spivack A. J. (2002) Metabolic activity of subsurface life in deep-sea sediments. *Science* **295**, 2067–2070.

Davis E. E., Chapman D. S., Wang K., Villinger H., Fisher A. T., Robinson S. W., Grigel J., Pribnow D., Stein J., and Becker K. (1999) Regional heat-flow variations across the sedimented Juan de Fuca Ridge eastern flank: Constraints on lithospheric cooling and lateral hydrothermal heat transport. *J. Geophys. Res.* **104,** *8*, 17675–17688.

Donnelly T. W., Pritchard R. A., Emmermann R., and Puchelt H. (1979) The aging of oceanic crust: Synthesis of the mineralogical and chemical results of Deep Sea Drilling Project, Legs 51 through 53. In *Initial Reports of the Deep Sea Drilling Project*, Vol. 51–53, part 2 (eds. T. W. Donnelly et al.), pp. 1563–1577. U.S. Government Printing Office.

Edwards K. J., Rogers D., Bach W., and McCollom T. M. (2002) A role for psychrophilic, rock-altering, chemolithoautotrophic Fe oxidizing bacteria in ocean crust weathering. *Eos* **83(47),** B22E-07.

Edwards K. J., Bach W., and Rogers D. (2003) Geomicrobiology of the ocean crust: A role for chemoautotrophic Fe-bacteria. *Biol. Bull.* **204**, 180–185.

Elderfield H. and Schultz A. (1996) Mid-ocean ridge hydrothermal fluxes and the chemical composition of the ocean. *Annu. Rev. Earth Planet. Sci.* **24**, 191–224.

Elderfield H., Wheat C. G., Mottl M. J., Monnin C., and Spiro B. (1999) Fluid and geochemical transport through oceanic crust: A transect across the eastern flank of the Juan de Fuca Ridge. *Earth Planet. Sci. Lett.* **172**, 151–165.

Emerson D. and Revsbech N. P. (1994) Investigation of an iron-oxidizing microbial mat community located near Aarhus, Denmark: Laboratory studies. *Appl. Environ. Microbiol.* **60**, 4032–4038.

Emerson D. and Moyer C. (1997) Isolation and characterization of novel iron-oxidizing bacteria that grow in circumneutral pH. *Appl. Environ. Microbiol.* **63**, 4784–4792.

Emerson D. and Moyer C. L. (2002) Neutrophilic Fe-oxidizing bacteria are abundant at the Loihi seamount hydrothermal vents and play a major role in Fe oxide deposition. *Appl. Environ. Microbiol.* **68**, 3085–3093.

Evans U. R. and Wanklyn J. N. (1946) Evolution of hydrogen from ferrous hydroxide. *Nature* **162**, 27–28.

Fein J. B., Daughney C. J., Yee N., and Davis T. (1997) A chemical equilibrium model of metal adsorption onto bacterial surfaces. *Geochim. Cosmochim. Acta* **61**, 3319–3328.

Fisher A. T. (1998) Permeability within basaltic oceanic crust. *Rev. Geophys.* **36**, 143–182.

Fisher A. T., Becker K., Narasimhan T. N., Langseth M. G., and Mottl M. J. (1990) Passive, off-axis convection through the southern flank of the Costa Rica Rift. *J. Geophys. Res.* **95**, 9343–9370.

Fisher A. T. and Becker K. (2000) Channelized fluid flow in oceanic crust reconciles heat-flow and permeability data. *Nature* **403**, 71–74.

Fisk M. R., Giovannoni S. J., and Thorseth I. H. (1998) The extent of microbial life in volcanic crust of the ocean basins. *Science* **281**, 978–980.

Furnes H. and Staudigel H. (1999) Biological mediation in ocean crust alteration: How deep is the deep biosphere. *Earth Planet. Sci. Lett.* **166**, 97–103.

Furnes H., Muehlenbachs K., Torsvik T., Thorseth I. H., and Tumyr O. (2001) Microbial fractionation of carbon isotopes in altered basaltic glass from the Atlantic Ocean, Lau Basin and Costa Rica Rift. *Chem. Geol.* **173**, 313–330.

German C. R., Baker E. T., Mevel C., Tamaki K., and Team F. S. (1998) Hydrothermal activity along the southwest Indian ridge. *Nature* **395**, 490–493.

German C. R., Klinkhammer G. P., Edmond J. M., Mitra A., and Elderfield H. (1990) Hydrothermal scavenging of rare-earth elements in the ocean. *Nature* **345**, 516–518.

Ghiorse W. C. (1984) Biology of iron- and manganese-depositing bacteria. *Ann. Rev. Microbiol.* **38**, 515–550.

Gillis K. M. and Robinson P. T. (1990) Patterns and processes of alteration in the lavas and dikes of the Troodos ophiolite, Cyprus. *J. Geophys. Res.* **95**, 21523–21548.

Gold T. (1992) The deep, hot biosphere. *Proc. Natl. Acad. Sci. USA* **89 (13),** 6045–6049.

Grevemeyer I. and Weigel W. (1997) Increase in seismic velocities of the uppermost oceanic crust versus age. *Geophys. Res. Lett.* **24**, 217–220.

Habicht K. S. and Canfield D. E. (2001) Isotope fractionation by sulfate-reducing natural populations and the isotopic composition of sulfide in marine sediments. *Geology* **29**, 555–558.

Hart S. R. and Staudigel H. (1982) The control of alkalies and uranium in seawater by ocean crust alteration. *Earth Planet. Sci. Lett.* **58**, 202–212.

Hart S. R. and Staudigel H. (1982) Ocean crust vein mineral deposition: Rb/Sr ages, U-Th-Pb geochemistry, and duration of circulation at DSDP sites 261, 462 and 516. *Geochim. Cosmochim. Acta* **50**, 2751–2761.

Heijnen J. J. and Van Dijken J. P. (1992) In search of a thermodynamic description of biomass yields for the chemotrophic growth of microorganisms. *Biotechnol. Bioengineer.* **39**, 833–858.

Hoehler T. M., Alperin M. J., Albert B., and Martens C. S. (1998) Thermodynamic control on hydrogen concentrations in anoxic sediments. *Geochim. Cosmochim. Acta* **62**, 1745–1756.

Hoehler T. M., Alperin M. J., Albert B., and Martens C. S. (2001) Apparent minimum free energy requirements for methanogenic Archaea and sulfate-reducing bacteria in an anoxic marine sediment. *FEMS Microbiol. Ecol.* **38**, 33–41.

Holloway J. R. and O'Day P. A. (2000) Production of CO_2 and H_2 by diking-eruptive events at mid-ocean ridges: Implications for abiotic organic synthesis and global geochemical cycling. *Int. Geol. Rev.* **42 (8),** 673–683.

Holm N. G. and Charlou J.-L. (2001) Initial indications of abiotic formation of hydrocarbons in the Rainbow ultramafic hydrothermal system, Mid-Atlantic Ridge. *Earth Planet. Sci. Lett.* **191**, 1–8.

Honnorez J. (1981) The aging of the oceanic crust at low temperature. In *The Sea*, Vol. 7 (ed. C. Emiliani), pp. 525–587. Wiley.

Hubberten H.-W. (1983) Sulfur content and sulfur isotopes of basalts from the Costa Rica Rift (Hole 504B, Deep Sea Drilling Project Legs 69 and 70). In *Initial Reports of the DSDP*, Vol. 69 (eds. J. R. Cann,

M. G. Langseth, J. Honnorez, R. P. Von Herzen, S. M. White, et al.), pp. 629–635. Deep Sea Drilling Program.

Jackson B. E. and McInerney M. J. (2002) Anaerobic microbial metabolism can proceed close to thermodynamic limits. *Nature* **415**, 454–456.

Jannasch H. W. (1995) Microbial interactions with hydrothermal fluids. In *Seafloor Hydrothermal Systems* (eds. S. E. Humphris, R. A. Zierenberg, L. S. Mullineaux, and R. E. Thomson), pp. 273–296. American Geophysical Union.

Johnson H. P. and Semyan S. W. (1994) Age variation in the physical properties of oceanic basalts: Implications for crustal formation and evolution. *J. Geophys. Res.* **99(B2),** 3123–3134.

Jones B., Renaut R. W., and Rosen M. R. (1997) Biogenicity of silica precipitation around geysers and hot spring vents, North Island, New Zealand. *J. Sediment. Res.* **67**, 88–104.

Juniper S. K. and Tebo B. M. (1995) Microbe-metal interactions and mineral deposition at hydrothermal vents. In *The Microbiology of Deep-Sea Hydrothermal Vents* (ed. D. M. Karl), pp. 219–253. CRC Press.

Juniper S. K. and Fouquet Y. (1988) Filamentous iron-silica deposits from modern and ancient hydrothermal sites. *Can. Min.* **26**, 859–869.

Karl D. M. (1995) Ecology of free-living, hydrothermal vent microbial communities. In *Microbiology of Deep-Sea Hydrothermal Vents* (ed. D. M. Karl), pp. 35–123. CRC Press.

Kelley D. S., Karson J. A., Blackman D. K., Früh-Green G. L., Butterfield D. A., Lilley M. D., Olson E. J., Schrenk M. O., Roe K. K., Lebon G. T., Rivizzigno P., and Party A.-S. (2001) An off-axis hydrothermal vent field near the Mid-Atlantic Ridge at 30 degrees N. *Nature* **412**, 127–128.

Kelley K. A., Plank T., Ludden J., and Staudigel H. (2003) The composition of altered oceanic crust at ODP Sites 801 and 1149. *Geochem. Geophys. Geosys.* **4,** *(6),* 10.1029/2002GC000435.

Konhauser K. O. and Ferris F. G. (1996) Diversity of iron and silica precipitation by microbial mats in hydrothermal waters, Iceland: Implications for Precambrian iron formations. *Geology* **24**, 323–326.

Krouse H. R., Brown H. M., and Farquharson R. B. (1977) Sulfur isotopic composition in DSDP Leg 37 cores. In *Initial Reports of the Deep Sea Drilling Project*, Vol. 37 (eds. F. Aumento et al.), pp. 621–623. U.S. Government Printing Office.

Kuenen J. G., Robertson L. A., and Touvinen O. H. (1992) The genera *Thiobacillus*, *Thiomicrospira*, and *Thiospera*. In *The Prokaryotes* (eds. A. Balows, H. G. Trüper, M. Dworkin, W. Harder, and K.-H. Schleifer), pp. 2638–2657. Springer-Verlag, Berlin.

Lecuyer C. and Yanick R. (1999) Long-term fluxes and budget of ferric iron: Implication for the redox state of the Earth's mantle and atmosphere. *Earth Planet. Sci. Lett.* **165**, 197–211.

Lovley D. R. and Chapelle F. H. (1995) Deep subsurface microbial processes. *Rev. Geophys.* **33**, 365–381.

Lovley D. R. and Goodwin S. (1988) Hydrogen concentrations as an indicator of the terminal electron-accepting reactions in aquatic sediments. *Geochim. Cosmochim. Acta* **52**, 2993–3003.

Lovley D. R., Philips E. J. P., Gorby Y. A., and Landa E. R. (1991) Microbial reduction of uranium. *Nature* **350**, 413–416.

Machel H. G. (2001) Bacterial and thermochemical sulfate reduction in diagenetic settings; old and new insights. *Sediment. Geol.* **140**, 143–175.

Marescotti P., Vanko D. A., and Cabella R. (2000) From oxidizing to reducing alteration: Mineralogical variations in pillow basalts from the east flank of the Juan de Fuca Ridge. In *Proceedings of the Ocean Drilling Program, Sci. Results 168* (eds. A. Fisher, E. E. Davis, and C. Escutia), pp. 119–136. Ocean Drilling Program.

Mathez E. A. (1976) Sulfur solubility and magmatic sulfides in submarine basalt glass. *J. Geophys. Res.* **81**, 4269–4275.

Mathez E. A. (1979) Sulfide relations in Hole 418A flows and sulfur contents of glasses. In *Initial Reports of the Deep Sea Drilling Project*, Vol. 51–53 (eds. T. Donnelly et al.), pp. 1069–1085. U.S. Government Printing Office.

McCollom T. M. (2000) Geochemical constraints on primary productivity in submarine hydrothermal vent plumes. *Deep-Sea Res. I* **47**, 85–101.

Melson W. G., O'Hearn T., and Jarosewitch E. (2002) A data brief on the Smithsonian Abyssal Volcanic Glass Data File. *Geochem. Geophys. Geosyst.* **3,** 10.1029/2001GC000249.

Mottl M. J. and Wheat C. G. (1994) Hydrothermal circulation through mid-ocean ridge flanks: Fluxes of heat and magnesium. *Geochim. Cosmochim. Acta* **58**, 2225–2237.

Neal C. and Stanger G. (1983) Hydrogen generation from mantle source rocks in Oman. *Earth Planet. Sci. Lett.* **66**, 315–320.

Noel M. (1985) Heat flow, sediment faulting and porewater advection in the Madeira anyssal plain. *Earth Planet. Sci. Lett.* **73**, 398–406.

Parsons B. (1981) The rates of plate creation and consumption. *Geophys. J. R. Astron. Soc.* **67**, 437–448.

Pederson K. (1997) Microbial life in granitic rock. *FEMS Microbiol. Rev.* **20**, 399–414.

Peterson C., Duncan R., and Scheidegger K. F. (1986) Sequence and longevity of basalt alteration at Deep Sea Drilling Project Site 597. In *Initial Reports of the Deep Sea Drilling Project 92* (eds. M. Leinen et al.), pp. 505–515. U.S. Government Printing Office.

Pezard P. A. and Anderson R. N. (1989) Morphology and alteration of the upper oceanic crust from in situ electrical experiments in DSDP/ODP Hole 504B. In *Proceedings of the Ocean Drilling Program, Sci. Results 111* (eds. K. Becker et al.), pp. 133–146. Ocean Drilling Program.

Rudnicki M. D., Elderfield H., and Spiro B. (2001) Fractionation of sulfur isotopes during bacterial sulfate reduction in deep ocean sediments at elevated temperatures. *Geochim. Cosmochim. Acta* **65**, 777–789.

Sansone F. J., Mottl M. J., Olson E. J., Wheat C. G., and Lilley M. D. (1998) CO_2-depleted fluids from mid-ocean ridge-flank hydrothermal springs. *Geochim. Cosmochim. Acta* **62**, 2247–2252.

Schink B. (1997) Energetics of syntropic coorperation in methanogenic degradation. *Microbiol. Mol. Biol. Rev.* **61**, 262–280.

Schippers A. and Sand W. (1999) Bacterial leaching of metal sulfides proceeds by two indirect mechanisms via thiosulfate or via polysulfides and sulfur. *Appl. Environ. Microbiol.* **65**, 319–321.

Schippers A. and Jørgensen B. B. (2001) Oxidation of pyrite and iron sulfide by manganese dioxide in marine sediment. *Geochim. Cosmochim. Acta* **65**, 915–922.

Schrag D. P. (1999) Carbon isotopic composition of dissolved inorganic carbon in deep sea pore fluids: Evidence for chemoautotrophy. *Geol. Soc. Am. Abstr.* **31**, 489.

Sclater J. G., Jaupart C., and Galson D. (1980) The heat flow through oceanic and continental crust and the heat loss of the Earth. *Rev. Geophys. Space Phys.* **18**, 269–311.

Shanks W. C. and Seyfried W. E. (1987) Stable isotope studies of vent fluids and chimney minerals, southern Juan de Fuca ridge: Sodium metasomatism and seawater sulfate reduction. *J. Geophys. Res.* **92**, 11387–11399.

Shock E. L. (1992) Chemical environments of submarine hydrothermal systems. In *Marine Hydrothermal Systems and the Origin of Life* (ed. N. G. Holm), pp. 67–107. Kluwer Academic.

Sørensen K. B., Finster K., and Ramsing N. B. (2001) Thermodynamic and kinetic requirements in anaerobic methane oxidizing consortia exclude hydrogen, acetate, and methanol as possible electron shuttles. *Microb. Ecol.* **42**, 1–10.

Staudigel H. and Hart S. R. (1983) Alteration of basaltic glass: Mechanisms and significance for the oceanic crust-seawater budget. *Geochim. Cosmochim. Acta* **47**, 337–350.

Staudigel H., Davies G. R., Hart S. R., Marchant K. M., and Smith B. M. (1995) Large scale isotopic Sr, Nd and O isotopic anatomy of altered oceanic crust: DSDP/ODP sites 417/418. *Earth Planet. Sci. Lett.* **130**, 169–185.

Staudigel H., Plank T., While B., and Schmincke H.-U. (1996) Geochemical fluxes during seafloor alteration of the basaltic upper oceanic crust: DSDP Sites 417 and 418. In *Subduction Top to Bottom* (eds. G. E. Bebout, D. W. Scholl, S. H. Kirby, and J. P. Platt), pp. 19–38. Geophysical Monograph 96. American Geophysical Union.

Stein C. A., Stein S., and Pelayo A. (1995) Heat flow and hydrothermal circulation. In *Seafloor Hydrothermal Processes* (eds. S. E. Humphris, R. A. Zierenberg, L. S. Mullineaux, and R. E. Thomson), pp. 425–445. American Geophysical Union.

Stein J. and Fisher A. T. (2000) Lateral hydrothermal circulation beneath the eastern flank of Juan De Fuca Ridge: Thermal, chemical and modeling constraints. *Eos Trans. Am. Geophys. Union.* **81**, F481.

Stevens T. O. and McKinley J. P. (1995) Lithoautotrophic microbial ecosystems in deep basalt aquifers. *Science* **270**, 450–454.

Stevens T. O. and McKinley J. P. (2000) Abiotic controls on H_2 production from basalt-water reactions and implications for aquifer biogeochemistry. *Environ. Sci. Technol.* **34**, 826–831.

Stevens T. O. and McKinley J. P. (2001) Response to comment on "Abiotic controls on H_2 production from basalt-water reactions and implications for aquifer biogeochemistry." *Environ. Sci. Technol.* **35**, 1558–1559.

Straub K. L., Benz M., Schink B., and Widdel F. (1996) Anaerobic, nitrate-dependent microbial oxidation of ferrous iron. *Appl. Environ. Microbiol.* **62**, 1458–1460.

Teagle D. A. H., Alt J. C., Bach W., Halliday A., and Erzinger J. (1996) Alteration of the upper ocean crust in a ridge flank hydrothermal up-flow zone: Mineral, chemical, and isotopic constraints from ODP Hole 896A. In *Proceedings of the Ocean Drilling Program, Sci. Results 148* (eds. J. C. Alt, H. Kinoshita, L. B. Stokking, and P. J. Michael), pp. 119–150. Ocean Drilling Program.

Thompson G. (1983) Basalt-seawater interaction. In *Hydrothermal Processes at Seafloor Spreading Centers* (eds. P. A. Rona, K. Bostrom, and K. L. Smith), pp. 225–278. Plenum.

Torsvik T., Furnes H., Muehlenbachs K., Thorseth I. H., and Tumyr O. (1998) Evidence for microbial activity at the glass-alteration interface in oceanic basalts. *Earth Planet. Sci. Lett.* **162**, 165–176.

Wallace P. and Carmichael I. S. E. (1992) Sulfur in basaltic magmas. *Geochim. Cosmochim. Acta* **56**, 1863–1874.

Wheat C. G. and Mottl M. J. (2000) Composition of pore and spring waters from baby bare: Global implications of geochemical fluxes from a ridge flank hydrothermal system. *Geochim. Cosmochim. Acta* **64**, 629–642.

Zhou W., Peacor D. R., Alt J. C., Van der Voo R., and Kao L.-S. (2001) TEM study of the alteration of interstitial glass in MORB by inorganic processes. *Chem. Geol* **174**, 365–376.

Zierenberg R. A. and Schiffman P. (1990) Microbial control of silver mineralization at a seafloor hydrothermal site on the northern Gorda Ridge. *Nature* **348**, 155–157.